C.P. No. 1137

C.P. No. 1137

MINISTRY OF AVIATION SUPPLY

AERONAUTICAL RESEARCH COUNCIL

CURRENT PAPERS

Subsonic Theoretical Lift-Curve Slope, Aerodynamic Centre and Spanwise Loading for Arbitrary Aspect Ratio, Taper Ratio and Sweepback

By

H. C. Garner and Sandra M. Inch
Aerodynamics Division NPL

LONDON: HER MAJESTY'S STATIONERY OFFICE

1971

PRICE 13s 0d [65p] net

C.P. No. 1137*
May 1970

Subsonic Theoretical Lift-Curve Slope, Aerodynamic Centre and Spanwise Loading for Arbitrary Aspect Ratio, Taper Ratio and Sweepback

- By -
H. C. Garner and Sandra M. Inch

SUMMARY

Full solutions by subsonic lifting-surface theory are tabulated for 64 planforms with systematic variation in aspect ratio, taper ratio and sweepback. The results indicate that existing data sheets incur errors of up to at least 7% in lift slope, 0·02 aerodynamic mean chord in aerodynamic centre and 0·012 semi-span in spanwise centre of pressure. With the aid of sonic theory and the usual similarity rules, alternative graphical presentations of the new data are discussed. A simple relationship between lift-dependent drag and spanwise centre of pressure is shown to hold within about 1%.

List of Contents/

---

* Replaces NPL Aero Report 1317 - A.R.C.32 143

List of Contents

List of Symbols/

List of Symbols

A	aspect ratio of wing; $2s/\bar{c}$
A_{2p-1}	coefficient of series for γ in equation (22)
$c(\eta)$	local chord of wing
c_r, c_t	root chord, tip chord of wing
$\bar{c}$	geometric mean chord of wing
$\bar{\bar{c}}$	aerodynamic mean chord in equation (3)
C_D	drag/$(\frac{1}{2}\rho U^2 S)$
C_L	lift/$(\frac{1}{2}\rho U^2 S)$
C_{LL}	local lift coefficient in equation (13)
C_m	pitching moment about $x = 0/(\frac{1}{2}\rho U^2 S\bar{c})$
K	trailing-vortex drag factor in equation (21)
$\ell(x,y)$	lift per unit area/$(\frac{1}{2}\rho U^2)$ in equation (10)
m	number of collocation sections (= 23)
M	Mach number of free stream
n	integer or subscript numerating loading station $\eta = \eta_n$
N	odd number of chordwise terms (= 3)
q	spanwise integration parameter (= 4)
s	semi-span of wing
S	area of wing planform; $2s\bar{c}$
U	uniform velocity of free stream
x,y	rectangular co-ordinates with origin at root leading edge
x_{ac}	value of x at aerodynamic centre
$x_\ell(\eta)$	leading edge of wing
$\bar{\bar{x}}_\ell$	$x_\ell(\bar{\bar{\eta}})$ in equation (5)
$\bar{x}$	aerodynamic centre in equation (6)

x_{ac}/

X_{ac}	local aerodynamic centre in equation (13)
z	integer $\frac{1}{2}(m-1)(= 11)$
α	uniform incidence of wing in radians
β	compressibility factor; $(1-M^2)^{\frac{1}{2}}$
γ, γ_n	first term in $\ell(x,y)$, its value at $\eta = \eta_n$
η, η_n	non-dimensional spanwise ordinate; y/s, $\sin[n\pi/(m+1)]$
$\bar{\eta}$	spanwise centre of pressure in equation (14)
$\bar{\bar{\eta}}$	section associated with $\bar{\bar{c}}$ in equation (4)
θ	angular spanwise position in equation (22)
κ_n	third term in $\ell(x,y)$ at section $\eta = \eta_n$
λ	taper ratio of wing; c_t/c_r
$\Lambda_{\frac{1}{2}}, \Lambda_1$	angle of sweepback of mid-chord line, trailing edge
μ_n	second term in $\ell(x,y)$ at section $\eta = \eta_n$
ρ	density of free stream
ϕ	angular chordwise position in equation (11)

1./

1. Introduction

The Royal Aeronautical Society has published in its series of Aerodynamic Data Sheets one set of charts for the linearized theoretical lift slope of thin wings (Ref. 1) and a similar set for the aerodynamic centre (Ref. 2). The wing planforms cover a wide range of straight taper, sweepback and aspect ratio and are considered in subsonic and supersonic flow. While the supersonic regime can largely be handled by direct computation from formulae that are exact within the assumptions of linear theory, the subsonic half of the Data Sheets relies on the approximate theories that were the best available some fifteen years ago. In view of recent improvements in subsonic lifting-surface theory, the accuracy of Refs. 1 and 2 has been examined in Ref. 3, where it is recommended that some revision is necessary for the larger angles of sweepback. It is considered that fairly simple modifications should suffice, but that further theoretical data would be necessary in the first place.

The present note provides a systematic set of theoretical solutions for the 64 planforms described in Section 3. The results, discussed in Sections 4 and 5, are currently being used to revise and extend the existing Data Sheets in Refs. 1 and 2. The complete solutions, tabulated for wings at uniform incidence, are available for more detailed analysis of local aerodynamic centres, for example. Charts for the spanwise centre of pressure and applications to spanwise loading and vortex drag are discussed in Section 6.

2. Existing Data Sheets

The family of straight tapered wings with streamwise tips is determined by three independent parameters, and those selected in the Data Sheets of Refs. 1 and 2 are

taper ratio λ , the ratio of tip chord to root chord,

aspect ratio A , the ratio of span to geometric mean chord,

$A \tan \Lambda_{\frac{1}{2}}$, twice the ratio of the streamwise extent of the mid-chord line to geometric mean chord.

By the well-known similarity rule for linearized inviscid steady flow, a uniform subsonic stream of arbitrary Mach number M can be included within the three-parameter framework. It is sufficient to multiply the lift and moment by the compressibility factor $\beta = (1-M^2)^{\frac{1}{2}}$ and to consider these reduced quantities as functions of λ, βA and $A \tan \Lambda_{\frac{1}{2}}$.

In Ref. 1, the ratio of reduced lift slope to reduced aspect ratio

$$\frac{\beta\, \partial C_L/\partial\alpha}{\beta A} = \frac{1}{A}\,\frac{\partial C_L}{\partial\alpha}$$

is presented graphically as a function of βA and $A \tan \Lambda_{\frac{1}{2}}$ for each

of/

of the taper ratios $\lambda = 1$, 0·5, 0·25 and 0. Linearized results for a sonic stream $(M \to 1)$ have little practical validity, but are included as the important limiting case $\beta A = 0$. The form of presentation is impeccable, and the shortcomings stem solely from inaccuracy in the basic calculations of lift slope.

Similar remarks apply to the presentation and accuracy of the charts in Ref. 2 for aerodynamic centre, defined as the point on the axis of symmetry of the wing about which the rate of change of pitching moment with incidence is zero. It is most easily expressed in terms of its distance downstream of the root leading edge as a fraction of geometric mean chord, so that

$$\frac{x_{ac}}{\bar{c}} = - \frac{\partial C_m/\partial\alpha}{\partial C_L/\partial\alpha} , \qquad \cdots (1)$$

where

$$\bar{c} = \int_0^1 c(\eta)\, d\eta = \tfrac{1}{2}(c_r + c_t) = \tfrac{1}{2}c_r(1 + \lambda) . \qquad \cdots (2)$$

The quantity $x_{ac}/\bar{c}$ varies over a wide range and is not an ideal ordinate for a graph. Moreover, it is customary to refer the aerodynamic centre to the aerodynamic mean chord

$$\bar{\bar{c}} = \frac{1}{\bar{c}} \int_0^1 [c(\eta)]^2\, d\eta = \frac{2c_r(1 + \lambda + \lambda^2)}{3(1 + \lambda)} , \qquad \cdots (3)$$

which is identified with the local chord at

$$\eta = \bar{\bar{\eta}} = \frac{1 + 2\lambda}{3(1 + \lambda)} \qquad \cdots (4)$$

with leading edge

$$x_\ell = \bar{\bar{x}}_\ell = \frac{(1 + 2\lambda)c_r}{12} \left[A \tan \Lambda_{\frac{1}{2}} + \frac{2(1 - \lambda)}{1 + \lambda} \right] . \qquad \cdots (5)$$

For any straight tapered wing with streamwise tips, the aerodynamic centre is then defined by the quantity

$$\frac{\bar{x}}{\bar{\bar{c}}} = \frac{x_{ac} - \bar{\bar{x}}_\ell}{\bar{\bar{c}}} = \frac{3(1 + \lambda)^2}{4(1 + \lambda + \lambda^2)} \frac{x_{ac}}{\bar{c}} - \frac{1 + 2\lambda}{8(1 + \lambda + \lambda^2)} \left[(1 + \lambda) A \tan \Lambda_{\frac{1}{2}} + 2(1 - \lambda) \right] , \qquad \cdots (6)$$

which normally lies in the range 0·15 to 0·50.

The/

The accuracy of the two sets of Data Sheets was investigated for ten planforms in Ref. 3, in Fig. 2 of which the errors are estimated to range between +2% and -6% in $\partial C_L/\partial\alpha$ (Ref. 1) and between ±0·02 in $\bar{x}/\bar{\bar{c}}$ (Ref. 2). In each case the worst errors are found when $A \tan \Lambda_{\frac{1}{2}} > 1{\cdot}5$. Extensive variation of this sweepback parameter is now essential.

3. Scope of Calculations

As explained in Section 1, the present investigation is confined to the subsonic half of the Data Sheets. Most of the calculations are for $\beta A > 0$, and the theoretical method is discussed briefly in Section 3.1 with equations for the load distribution and the derived aerodynamic data. The limiting case $\beta A = 0$ is considered analytically and numerically, as outlined in Section 3.2.

The chosen planforms correspond to parametric values

$$\left.\begin{aligned} \lambda &= 1,\ 0{\cdot}5,\ 0{\cdot}25 \text{ and } 0 \\ \beta A &= 8,\ 5,\ 3 \text{ and } 1{\cdot}5 \\ A \tan \Lambda_{\frac{1}{2}} &= 0,\ 2,\ 4 \text{ and } 6 \end{aligned}\right\}, \qquad \ldots (7)$$

the additional case $\beta A = 0$ being considered separately. The 64 planforms, numbered and defined in Table 1, may be regarded as lying on or inside a cube such that each parameter is represented by a principal axis. Twelve planforms, one from each edge of the cube, are illustrated in Fig. 1.

3.1 Subsonic theory

The basic method is that described in detail in Ref. 4, with the simplification that the frequency is zero to give steady flow. The method is strictly applicable to planforms with smooth perimeter. While the corners of a streamwise tip raise no practical difficulties, the kink at the centre of a swept or tapered wing cannot be accommodated and some artificial rounding is necessary. The convergence and accuracy of the method are discussed in Ref. 5 for a variety of planforms. Given the aerodynamic problem, we can vary the following arbitrary quantities in the numerical solution:

N, the number of chordwise terms or collocation positions;

m, the odd number of collocation sections between the tips;

$q(m+1)-1$, the number of spanwise integration points;

the spanwise extent and shape of artificial central rounding.

Sufficient convergence with respect to q and N can usually be established, while that with respect to m can be facilitated by an increase in the amount of rounding. Experience from Ref. 5 shows that $N = 3$ should be enough to give the lift slope, spanwise loading and aerodynamic centre to the desired accuracy; moreover,

$$q(m+1) = 96$$

should/

should provide satisfactory spanwise integration, and we choose $m = 23$ and $q = 4$. The artificial rounding can then be limited to the region

$$|\eta| < \eta_1 = \sin\frac{\pi}{m+1} = 0{\cdot}13053 \,, \qquad \cdots (8)$$

provided that the shape of rounding is taken from Ref. 6, that is, from equations (48) of Ref. 5

$$\left.\begin{aligned} x_\ell(\eta) &= x_\ell(\eta_1)\left[\tfrac{1}{3} + (|\eta|/\eta_1)^2 - \tfrac{1}{3}(|\eta|/\eta_1)^3\right] \\ c(\eta) &= c_r + \left[\tfrac{1}{3} + (|\eta|/\eta_1)^2 - \tfrac{1}{3}(|\eta|/\eta_1)^3\right]\left\{c(\eta_1) - c_r\right\} \end{aligned}\right\} . \qquad \cdots (9)$$

Some checks on accuracy will be described in Section 4 before the discussion of the main calculations with $N = 3$, $m = 23$, $q = 4$ and the NLR rounding from equations (8) and (9).

The solutions consist of numerical coefficients γ_n, μ_n and κ_n that define the load distributions at the collocation sections $\eta = \eta_n$ with $n = 0, 1, \ldots \tfrac{1}{2}(m-1)$

$$\frac{\Delta p}{\tfrac{1}{2}\rho U^2} = \ell(x,y) = \frac{8s}{\pi c_n}\Big[\gamma_n \cot\tfrac{1}{2}\phi + 4\mu_n(\cot\tfrac{1}{2}\phi - 2\sin\phi)$$
$$+ \kappa_n(\cot\tfrac{1}{2}\phi - 2\sin\phi - 2\sin 2\phi)\Big] , \qquad \cdots (10)$$

where

$$\left.\begin{aligned} x &= x_\ell(\eta_n) + \tfrac{1}{2}c(\eta_n)(1 - \cos\phi) \\ &= x_{\ell n} + \tfrac{1}{2}c_n(1 - \cos\phi) \\ y &= s\sin[n\pi/(m+1)] \end{aligned}\right\} . \qquad \cdots (11)$$

Hence the lift and pitching moment about the root leading edge are obtained as

C_L/

$$\left.\begin{aligned} C_L &= \frac{\pi A}{m+1} \sum_{n=-z}^{z} \gamma_n \cos \frac{n\pi}{m+1} \qquad [z = \tfrac{1}{2}(m-1)] \\ -C_m &= \frac{\pi A}{m+1} \sum_{n=-z}^{z} \frac{1}{\bar{c}} \left\{ \gamma_n (x_{\ell n} + \tfrac{1}{4} c_n) - \mu_n c_n \right\} \cos \frac{n\pi}{m+1} \end{aligned}\right\} \quad \ldots (12)$$

The aerodynamic centre can then be evaluated from equations (1) and (6). If required, the local lift coefficient and aerodynamic centre at $\eta = \eta_n$ are given by

$$\left.\begin{aligned} C_{LL} &= \frac{\text{Lift per unit span}}{\tfrac{1}{2}\rho U^2 c_n} = \frac{4s\gamma_n}{c_n} \\ x &= x_{\ell n} + X_{ac}\, c_n \quad \text{with} \quad X_{ac} = \frac{1}{4} - \frac{\mu_n}{\gamma_n} \end{aligned}\right\} \quad \ldots (13)$$

With symmetrical spanwise loading, the spanwise centre of pressure on the half wing is

$$\bar{\eta} = \int_0^1 \frac{c\, C_{LL}}{\bar{c}\, C_L} \eta \, d\eta = \frac{2A}{C_L} \int_0^1 \gamma \eta \, d\eta$$

$$= \frac{2\pi A}{(m+1) C_L} \sum_{n=0}^{z} f_n \gamma_n \, , \quad \ldots (14)$$

where for $m = 23$

$$\left.\begin{aligned} f_0 &= 0{\cdot}01329 & f_4 &= 0{\cdot}43331 & f_8 &= 0{\cdot}43307 \\ f_1 &= 0{\cdot}12630 & f_5 &= 0{\cdot}48277 & f_9 &= 0{\cdot}35351 \\ f_2 &= 0{\cdot}25108 & f_6 &= 0{\cdot}50013 & f_{10} &= 0{\cdot}25003 \\ f_3 &= 0{\cdot}35303 & f_7 &= 0{\cdot}48288 & f_{11} &= 0{\cdot}12939 \end{aligned}\right\}$$

A numerical analysis of $\bar{\eta}$ is given in Section 6.

3.2 Sonic theory

Mangler's[7] theory for wings of arbitrary taper and sweepback at sonic speeds provides the lift slope and aerodynamic centre in the limit as $\beta A \to 0$. Although fair accuracy can be obtained by reading from the graph of lift slope in Fig. 11 of Ref. 7, the aerodynamic centre $\bar{x}/\bar{\bar{c}}$ from equation (6) is too sensitive to be determined satisfactorily from Fig. 12 of Ref. 7.

When the tip leading edge is not upstream of the root trailing edge, that is, when $A \tan \Lambda_{\frac{1}{2}} \leq 2$, there are simple analytical results

$$\left.\begin{aligned} \frac{1}{A}\frac{\partial C_L}{\partial \alpha} &= \tfrac{1}{2}\pi \\ \frac{x_{ac}}{\bar{c}} &= \tfrac{1}{3} A \tan \Lambda_{\frac{1}{2}} + \frac{2(1-\lambda)}{3(1+\lambda)} \end{aligned}\right\} . \qquad \ldots (15)$$

By equations (6) and (15)

$$\frac{\bar{x}}{\bar{\bar{c}}} = \frac{1}{8(1+\lambda+\lambda^2)} \left[(1+\lambda) A \tan \Lambda_{\frac{1}{2}} + 2(1-\lambda) \right] . \qquad \ldots (16)$$

In these simple cases the spanwise loading for a uniform incidence is elliptic and

$$\bar{\eta} = \frac{4}{3\pi} = 0{\cdot}42441 \; . \qquad \ldots (17)$$

When $A \tan \Lambda_{\frac{1}{2}} > 2$, equations (54) and (55) and Table 1 of Ref. 7 have been used to check the lift slope and to calculate the aerodynamic centre in a few special cases, namely for untapered wings and when the wing span is twice the local span through the root trailing edge. Results in other cases have been approximated by means of equation (117) of Ref. 7, but without the approximation in equation (118). With the single substitution

$$H(s) = (1-\sigma^2)^{-\frac{1}{2}} \text{ with } \sigma \text{ from equation (116) of Ref. 7,}$$

equations (54) and (55) of Ref. 7 have been evaluated, and hence approximate values of

$$\frac{1}{A}\frac{\partial C_L}{\partial \alpha} = \frac{C_L}{A\alpha}$$

and

$$\frac{x_{ac}}{\bar{c}} = -\frac{C_m}{C_L} .$$

These/

These results prove to be compatible with those for non-zero values of βA, as calculated by the method considered in Section 3.1.

4. Results and Comparisons

As discussed in Section 3.1, the method of Ref. 4 has been applied to each of the 64 planforms defined in Table 1 and equations (7). Although it is not possible to establish the absolute accuracy of these calculations with $(m,N,q) = (23,3,4)$, two possible limitations have been examined. In view of the recommended condition (41) in Ref. 5, which becomes $m \geqslant 39$ for Wing 4 at $M = 0$, it is necessary to check that $m = 23$ will suffice for present purposes. With the NLR rounding, defined in equations (8) and (9), the following values of lift slope and aerodynamic centre are calculated for Wing 4.

$\lambda = 1,\ \beta A = 8,\ A \tan \Lambda_{\frac{1}{2}} = 6$			$\frac{1}{A}\frac{\partial C_L}{\partial \alpha}$	$\frac{\bar{x}}{\bar{\bar{c}}}$
m	N	q		
15	3	4	0·4949	0·1762
15	3	8	0·4925	0·1782
23	3	4	0·4903	0·1774
31	3	2	0·4912	0·1751

The error in lift slope would appear to be less than 1%, and that in aerodynamic centre is of order $0{\cdot}002\,\bar{\bar{c}}$; these are acceptable under the extreme condition $\beta A = 8$. The other limitation arises not so much as an error but as a consequence of the large magnitude of artificial rounding when the sweepback is very high. The following table gives the results for four wings of low reduced aspect ratio $\beta A = 1{\cdot}5$ and shows the detrimental effect of increasing the NLR rounding by taking $m = 15$ in place of $m = 23$.

Wing	$\beta A = 1{\cdot}5$		$\frac{1}{A}\frac{\partial C_L}{\partial \alpha}$		$\bar{x}/\bar{\bar{c}}$	
	λ	$A \tan \Lambda_{\frac{1}{2}}$	m,N,q 15,3,8	m,N,q 23,3,4	m,N,q 15,3,8	m,N,q 23,3,4
14	1	2	1·2365	1·2324	0·1668	0·1654
15	1	4	0·9636	0·9520	0·1748	0·1740
16	1	6	0·7471	0·7376	0·1897	0·1889
48	0·25	6	0·7792	0·7736	0·4438	0·4387

The/

The order of uncertainty in lift slope is 1%, and it is considered that this could reach 2% in the most extreme cases; for rectangular wings, on the other hand, the errors are known to be less than ¼%. The discrepancies in aerodynamic centre are greatest for the tapered wing and might possibly be as high as $0{\cdot}01\bar{\bar{c}}$ in the extreme cases that arise when taper ratio, aspect ratio, sweepback and Mach number are all large.

For the limit $\beta A = 0$, equations (15) to (17) are exact, provided that $A \tan \Lambda_{\frac{1}{2}} \leqslant 2$. The approximate calculations for $A \tan \Lambda_{\frac{1}{2}} > 2$ give values of the lift slope within 2% of those estimated from the graph in Fig. 11 of Ref. 7; the accuracy of the aerodynamic centre cannot be guaranteed within $0{\cdot}01\bar{\bar{c}}$, but the comparisons between the results of the subsonic and sonic theories encourage the view that errors are confined to this order of magnitude.

Table 1 gives the subsonic lift and pitching moment for all 64 wings from the calculations with $(m,N,q) = (23,3,4)$ and the NLR rounding from equations (8) and (9). For comparison with the Data Sheets of Ref. 1, $(1/A)\,\partial C_L/\partial\alpha$ is included. The aerodynamic centre is presented both as $x_{ac}/\bar{c}$ from equation (1) and as $\bar{x}/\bar{\bar{c}}$ from equation (6) to compare with the quantity read from the Data Sheets of Ref. 2. The corresponding results for $\beta A = 0$ are listed in Table 2. The complete solutions for the nominal incidence $\alpha = 1$ radian are tabulated for Wings 1 to 16 of taper ratio $\lambda = 1$ in Table 3, and respectively for taper ratios $\lambda = 0{\cdot}5$, $0{\cdot}25$ and 0 in Tables 4, 5 and 6. The spanwise centre of pressure $\bar{\eta}$ has been evaluated from equation (14) in each case, and equations (10) and (13) are available for more detailed calculations.

The conclusions in Ref. 3 about the theoretical inaccuracy of the Data Sheets can be confirmed by analysis for the 64 wings. The estimated percentage errors in lift slope, calculated as

$$100 \left[\frac{\partial C_L/\partial\alpha \ \text{ from Data Sheet}}{\partial C_L/\partial\alpha \ \text{ from theory}} - 1 \right],$$

are plotted in Fig. 2 and range from +2·5% for Wing 33 to −9·1% for Wing 12 or 16. The latter is probably an exaggeration, because the artificial central rounding gives a fictitious increase in lift slope, which could be as much as 2% when $A \tan \Lambda_{\frac{1}{2}}$ is large. Nevertheless, the doubts raised in Fig. 2 of Ref. 3 are fully substantiated and the errors are thought to reach at least 7%. The corresponding differences in aerodynamic centre,

$$(\bar{x}/\bar{\bar{c}})_{\text{Data Sheet}} - (\bar{x}/\bar{\bar{c}})_{\text{theory}} ,$$

are obtainable for $A \tan \Lambda_{\frac{1}{2}} \leqslant 4$ and, ranging from +0·023 for Wing 20 to −0·027 for Wing 39, they are again consistent with Fig. 2 of Ref. 3. The analysis is summarized in Table 7, which shows how the estimated errors are distributed among each set of 16 wings having constant $A \tan \Lambda_{\frac{1}{2}}$. The

lift/

lift slope from Ref. 1 is a fair approximation for low sweepback, but progressively underestimates $\partial C_L/\partial\alpha$ as $A \tan \Lambda_{\frac{1}{2}}$ increases. On the other hand, the aerodynamic centre from Ref. 2 tends to lie aft of the theoretical position when $A \tan \Lambda_{\frac{1}{2}} = 0$; however, as the sweepback increases, the pattern of error changes to give diverging positive and negative discrepancies. The results in Tables 1 and 2 are therefore being used to provide new Data Sheets to supersede those in Refs. 1 and 2.

5. Graphical Presentations

The lift slope shows less dependence on taper ratio λ than on reduced aspect ratio βA or the sweepback parameter $A \tan \Lambda_{\frac{1}{2}}$. As in Ref. 1, charts with constant λ and variable βA and $A \tan \Lambda_{\frac{1}{2}}$ are quite serviceable. It is instructive to compare alternative presentations in carpet form with constant $\lambda = 0{\cdot}25$, constant $\beta A = 5$ and constant $A \tan \Lambda_{\frac{1}{2}} = 2$ in Figs. 3, 4 and 5 respectively. Fig. 3 is indeed the only well-balanced carpet. Broken lines are necessary in the upper part of Fig. 4, where the effects of λ and $A \tan \Lambda_{\frac{1}{2}}$ are both small and the curves overlap; this offsets any advantage of the larger scale of $(1/A)\,\partial C_L/\partial\alpha$. Fig. 4 also illustrates the need to include an extra taper ratio between 0 and 0·25. Figs. 3 and 5 both show a satisfactory link between subsonic theory $(\beta A \geqslant 1{\cdot}5)$ and sonic theory $(\beta A = 0)$. Nevertheless, it is the intermediate region where the uncertainties are greatest.

Corresponding carpets of the aerodynamic centre from equation (6) are drawn in Figs. 6, 7 and 8. The quantity $\bar{x}/\bar{\bar{c}}$ shows less dependence on βA than on the other two parameters, but it is clear from the lower part of Fig. 7 that charts for constant βA are impracticable. Figs. 6 and 8 provide equally good graphical presentations for $\lambda = 0{\cdot}25$ and $A \tan \Lambda_{\frac{1}{2}} = 2$, and they again illustrate the satisfactory link between the subsonic and sonic theories. The carpets for constant $A \tan \Lambda_{\frac{1}{2}}$ and abscissa $(\beta A + 4\lambda)$ remain open over the whole range of sweepback. On the other hand, difficulty is experienced with overlapping curves if a carpet for the constant taper ratio $\lambda = 1$ is attempted. It follows that Fig. 8 is the most suitable presentation of subsonic aerodynamic centre. Moreover, the subsequent interpolation in $A \tan \Lambda_{\frac{1}{2}}$ is so simple that the linear formula will suffice with unit intervals in $A \tan \Lambda_{\frac{1}{2}}$.

6. Spanwise Centre of Pressure

The approximate evaluation of $\bar{\eta}$, the spanwise centre of pressure, is a preliminary step in the rapid estimation of spanwise loading in Ref. 8. The results in Tables 3 to 6 with the aid of equation (14) are reasonably consistent with Figs. 1 and 2 of Ref. 8 corresponding to wings with unswept trailing edges, but there are minor differences up to ±0·002. The results for pointed tips $(\lambda = 0)$ in Table 6 enable the method of Ref. 8 to be extended over the whole range of taper, if desired. When the method is applied to the 48 wings with non-zero tip chord, the differences

$$(\bar{\eta})_{\text{Ref. 8}} - (\bar{\eta})_{\text{theory}}$$

range/

range from +0·012 for Wing 48 to -0·011 for Wing 16; however, as Table 8 shows, for 30 of the wings $\bar{\eta}$ from Ref. 8 is correct within ±0·002. The chart in Fig. 3 of Ref. 8 implies that $\bar{\eta}$ is a linear function of $A \tan \Lambda_{\frac{1}{2}}$ when βA and λ are held constant. The carpet of $\bar{\eta}$ for $\lambda = 0{\cdot}25$ in Fig. 9 shows that this approximation is unreliable when $A \tan \Lambda_{\frac{1}{2}} > 4$. Even the theoretical data for $A \tan \Lambda_{\frac{1}{2}} \leqslant 4$ would call for such revision of Fig. 3 of Ref. 8, that a data sheet for $\bar{\eta}$ on the lines of Refs. 1 and 2 is a preferable alternative. Figs. 10 and 11 illustrate carpets for constant βA and for constant $A \tan \Lambda_{\frac{1}{2}}$; they each emphasize how sensitive $\bar{\eta}$ is to taper ratio in the range $0 < \lambda < 0{\cdot}25$. For ease of interpolation, therefore, carpets for constant $A \tan \Lambda_{\frac{1}{2}}$, rather than constant λ, are recommended. Since information on $\bar{\eta}$ is lacking with both $\beta A < 1{\cdot}5$ and $A \tan \Lambda_{\frac{1}{2}} > 2$, there are arguments in favour of carpets for constant βA; these would all be complete and, with the proviso that $A > \beta A$, each could be applied to any practical straight-tapered wing at some particular subsonic Mach number.

Given an accurate chart for $\bar{\eta}$, it remains to check the formula from Ref. 8

$$\frac{cC_{LL}}{\bar{c}\,C_L} = F(\eta,\bar{\eta}) + (A \tan \Lambda_1)\,G(\eta) + (\beta A - 4)(1 + 3{\cdot}5\,\beta^{-1} \tan \Lambda_1)\,H(\eta)\,, \qquad \ldots (18)$$

where the last term is omitted if $\beta A < 4$, the trailing-edge sweepback parameter

$$A \tan \Lambda_1 = A \tan \Lambda_{\frac{1}{2}} - \frac{2(1-\lambda)}{1+\lambda}\,, \qquad \ldots (19)$$

and the functions $F(\eta,\bar{\eta})$, $G(\eta)$ and $H(\eta)$ are defined and plotted in Ref. 8. By equation (13) for C_{LL}

$$\frac{cC_{LL}}{\bar{c}C_L} = \frac{2A\,\gamma_n}{C_L} \quad \text{at} \quad \eta = \sin\frac{n\pi}{m+1} \qquad \ldots (20)$$

may be calculated from the solutions in Tables 3 to 6. Wings 16 and 49 are taken as extreme examples in Fig. 12, where the theoretical spanwise loading from equation (20) is compared with that from equation (18) when the theoretical value of $\bar{\eta}$ is substituted. Neither the combination of lowest aspect ratio and highest sweepback nor that of highest aspect ratio and full taper invalidates the formula of Ref. 8 to any great extent.

A/

A final enquiry is made into the validity of the approximate formula for trailing-vortex drag in Ref. 9

$$K = \frac{\pi A C_D}{C_L^2} = 1 + 46{\cdot}264\,(\bar{\eta} - 0{\cdot}42441) \quad . \qquad \cdots (21)$$

On writing the non-dimensional circulation γ in the form

$$\gamma = \sum_{p=1}^{\infty} A_{2p-1} \sin(2p-1)\theta \quad \text{with} \quad \eta = \cos\theta \ , \qquad \cdots (22)$$

it is easily shown from the integrals in Ref. 9 that

$$K = \sum_{p=1}^{\infty} (2p-1)(A_{2p-1}/A_1)^2 \ , \qquad \cdots (23)$$

where

$$A_{2p-1} = \frac{4}{\pi} \int_0^{\pi/2} \gamma \sin(2p-1)\theta \, d\theta$$

$$= \frac{4}{m+1} (-1)^{p-1} \left[\tfrac{1}{2}\gamma_0 + \sum_{n=1}^{z} \gamma_n \cos \frac{(2p-1)n\pi}{m+1} \right] . \qquad \cdots (24)$$

Equation (23) is found to give a rapidly convergent series for the vortex-drag factor K, which has been evaluated for wings of extreme planform. Equation (21) makes the approximation that $A_{2p-1} = 0$ for $p \geqslant 3$, and the two results are compared in the following table.

Wing	λ	βA	$A \tan \Lambda_{\frac{1}{2}}$	$\bar{\eta}$	Values of K	
					Eqn.(21)	Eqn.(23)
16	1·00	1·5	6	0·4786	1·136	1·131
32	0·50	1·5	6	0·4619	1·065	1·064
48	0·25	1·5	6	0·4470	1·024	1·026
64	0	1·5	6	0·4081	1·012	1·019
52	0	8·0	6	0·3887	1·059	1·070
49	0	8·0	0	0·3744	1·120	1·119

It/

It may be concluded that for straight-tapered wings equation (21) is reliable within about ±1%, even when $A \tan \Lambda_{\frac{1}{2}} = 6$.

7. Conclusions

(1) The Data Sheets of Refs. 1 and 2 are being revised on the basis of the present calculations. In cases of high sweepback, reductions of up to 7% in lift slope and corrections of $\pm 0{\cdot}02\bar{\bar{c}}$ in aerodynamic centre are necessary.

(2) The lift slope is best presented in carpet form with curves of $(1/A)\, \partial C_L/\partial\alpha$ against βA and $A \tan \Lambda_{\frac{1}{2}}$ for constant taper ratio λ. Apart from the range $0 < \lambda < 0{\cdot}25$, interpolation in λ is simple, as the lift slope shows least dependence on this parameter.

(3) The aerodynamic centre is best presented in carpet form with curves of $\bar{x}/\bar{\bar{c}}$ against βA and λ for constant sweepback parameter $A \tan \Lambda_{\frac{1}{2}}$. Linear interpolation will suffice with unit intervals in $A \tan \Lambda_{\frac{1}{2}}$.

(4) The rapid method in Ref. 8 for estimating spanwise loading due to wing incidence remains satisfactory, apart from the inadequacy of the charts for spanwise centre of pressure in cases of high sweepback. Carpet presentation of $\bar{\eta}$ is recommended, either as for $\bar{x}/\bar{\bar{c}}$ above, or for constant reduced aspect ratio βA.

(5) With the extended range of taper ratio, aspect ratio and sweepback, the approximate relationship $K(\bar{\eta})$ from Ref. 9 and in equation (21) continues to give the vortex-drag factor within about ±1%.

(6) The full solutions in Tables 3 to 6 are available for further analysis of spanwise loading and local aerodynamic centre, as defined in equations (13).

References/

References

No.	Author(s)	Title, etc.
1	Royal Aeronautical Society	Theoretical slope of lift curve for wings at high speed. Aerodynamics Data Sheets WINGS S.01.03.03 to 06. May, 1954.
2	Royal Aeronautical Society	Theoretical aerodynamic centre of swept and tapered wings at high speeds. Aerodynamics Data Sheet WINGS S.08.01.02. November, 1955.
3	H. C. Garner	Review of Royal Aeronautical Society Aerodynamics Data Sheets in the light of recent improvements in subsonic lifting-surface theory. N.P.L. Aero Note 1079. A.R.C.31 062. March, 1969.
4	H. C. Garner and D. A. Fox	Algol 60 programme for Multhopp's low-frequency subsonic lifting-surface theory. A.R.C. R.& M.3517. April, 1966.
5	H. C. Garner	Numerical appraisal of Multhopp's low-frequency subsonic lifting-surface theory. A.R.C. R.& M.3634 October, 1968.
6	P. J. Zandbergen, Th. E. Labrujere and J. G. Wouters	A new approach to the numerical solution of the equation of subsonic lifting surface theory. N.L.R. Report TR G.49. November, 1967.
7	K. W. Mangler	Calculation of the pressure distribution over a wing at sonic speeds. A.R.C. R.& M.2888. September, 1951.

8/

No.	Author(s)	Title, etc.
8	Royal Aeronautical Society	Method for the rapid estimation of theoretical spanwise loading due to a change of incidence. Transonic Data Memo. 6403. March, 1964.
9	H. C. Garner	Some remarks on vortex drag and its spanwise distribution in incompressible flow. Aeronaut. J.(R.Ae.S.)Vol.72, pp.623-625. July, 1968.

Table 1/

Table 1

Subsonic Theoretical Lift Slopes and Aerodynamic Centres of 64 Wings

WING	λ	βA	$A\tan\Delta_{\frac{1}{2}}$	$\beta \frac{\partial C_L}{\partial \alpha}$	$-\beta \frac{\partial C_m}{\partial \alpha}$	$\frac{1}{A} \frac{\partial C_L}{\partial \alpha}$	$\frac{x_{ac}}{\bar{c}}$	$\frac{\bar{x}}{\bar{\bar{c}}}$
1	1.0	8.0	0	4.594	1.110	0.574	0.242	0.242
2			2	4.501	3.156	0.563	0.701	0.201
3			4	4.254	5.025	0.532	1.181	0.181
4			6	3.922	6.579	0.490	1.677	0.177
5		5.0	0	3.957	0.934	0.791	0.236	0.236
6			2	3.804	2.628	0.761	0.691	0.191
7			4	3.430	4.030	0.686	1.175	0.175
8			6	2.995	5.032	0.599	1.680	0.180
9		3.0	0	3.146	0.707	1.049	0.225	0.225
10			2	2.946	1.998	0.982	0.678	0.178
11			4	2.490	2.916	0.830	1.171	0.171
12			6	2.047	3.446	0.682	1.684	0.184
13		1.5	0	2.022	0.393	1.348	0.195	0.195
14			2	1.849	1.230	1.232	0.665	0.165
15			4	1.428	1.676	0.952	1.174	0.174
16			6	1.106	1.869	0.738	1.689	0.189
17	0.5	8.0	0	4.736	1.888	0.592	0.399	0.242
18			2	4.640	3.917	0.580	0.844	0.243
19			4	4.385	5.728	0.548	1.306	0.260
20			6	4.041	7.188	0.505	1.779	0.287
21		5.0	0	4.072	1.600	0.814	0.393	0.236
22			2	3.919	3.312	0.784	0.845	0.244
23			4	3.539	4.663	0.708	1.317	0.270
24			6	3.093	5.563	0.619	1.799	0.306
25		3.0	0	3.216	1.224	1.072	0.381	0.224
26			2	3.022	2.561	1.007	0.848	0.246
27			4	2.568	3.419	0.856	1.331	0.284
28			6	2.118	3.845	0.706	1.816	0.322
29		1.5	0	2.040	0.714	1.360	0.350	0.195
30			2	1.881	1.609	1.254	0.855	0.253
31			4	1.473	1.989	0.982	1.350	0.302
32			6	1.147	2.099	0.765	1.829	0.335

Table 1 (contd.)/

Table 1 (contd.)

Subsonic Theoretical Lift Slopes and Aerodynamic Centres of 64 Wings

WING	λ	βA	$A\tan\Delta_{\frac{1}{2}}$	$\beta \frac{\partial C_L}{\partial \alpha}$	$-\beta \frac{\partial C}{\partial \alpha}$	$\frac{1}{A} \frac{\partial C_L}{\partial \alpha}$	$\frac{x_{ac}}{\bar{c}}$	$\frac{\bar{x}}{\bar{c}}$
33	0.25	8.0	0	4.755	2.465	0.594	0.518	0.249
34			2	4.660	4.433	0.582	0.951	0.278
35			4	4.406	6.155	0.551	1.397	0.319
36			6	4.064	7.510	0.508	1.848	0.364
37		5.0	0	4.082	2.100	0.816	0.515	0.245
38			2	3.931	3.788	0.786	0.963	0.289
39			4	3.556	5.062	0.711	1.423	0.342
40			6	3.112	5.859	0.622	1.882	0.395
41		3.0	0	3.212	1.623	1.071	0.505	0.237
42			2	3.026	2.964	1.009	0.980	0.303
43			4	2.583	3.750	0.861	1.452	0.368
44			6	2.135	4.078	0.712	1.910	0.420
45		1.5	0	2.026	0.978	1.351	0.483	0.217
46			2	1.881	1.891	1.254	1.006	0.327
47			4	1.484	2.203	0.990	1.484	0.397
48			6	1.160	2.241	0.774	1.931	0.439
49	0	8.0	0	4.543	3.092	0.568	0.681	0.260
50			2	4.458	4.818	0.557	1.081	0.311
51			4	4.232	6.296	0.529	1.488	0.366
52			6	3.925	7.433	0.491	1.894	0.420
53		5.0	0	3.863	2.636	0.773	0.682	0.262
54			2	3.730	4.143	0.746	1.111	0.333
55			4	3.398	5.218	0.680	1.536	0.402
56			6	2.999	5.841	0.600	1.948	0.461
57		3.0	0	3.026	2.066	1.009	0.683	0.262
58			2	2.860	3.286	0.953	1.149	0.362
59			4	2.463	3.906	0.821	1.585	0.439
60			6	2.056	4.092	0.685	1.991	0.493
61		1.5	0	1.922	1.310	1.281	0.682	0.261
62			2	1.785	2.150	1.190	1.205	0.403
63			4	1.421	2.325	0.947	1.636	0.477
64			6	1.119	2.263	0.746	2.022	0.516

Table 2/

Table 2

Approximate Lift Slopes and Aerodynamic Centres when $\beta A \to 0$

λ	$A \tan \Lambda_{\frac{1}{2}}$	$\frac{1}{A}\frac{\partial C_L}{\partial \alpha}$	$\frac{x_{ac}}{\bar{c}}$	$\frac{\bar{x}}{\bar{\bar{c}}}$
1·00	0	1·571	0	0
	2	1·571	0·667	0·167
	4	1·026	1·182	0·182
	6	0·752	1·702	0·202
0·50	0	1·571	0·222	0·071
	2	1·571	0·889	0·286
	4	1·079	1·375	0·326
	6	0·801	1·852	0·358
0·25	0	1·571	0·400	0·143
	2	1·571	1·067	0·381
	4	1·085	1·517	0·426
	6	0·810	1·958	0·462
0	0	1·571	0·667	0·250
	2	1·571	1·333	0·500
	4	1·048	1·684	0·513
	6	0·785	2·052	0·539

Table 3/

Table 3

Solutions with $\lambda = 1$, $(m,N,q) = (23,3,4)$, NLR Rounding, $M = 0$, $\alpha = 1$

WING A $A\tan\Lambda_{\frac{1}{2}}$	1 8 0	2 8 2	3 8 4	4 8 6	5 5 0	6 5 2
γ_0	0.33372	0.30690	0.27404	0.24139	0.47504	0.42193
γ_1	0.33261	0.31161	0.28258	0.25177	0.47272	0.42829
γ_2	0.32916	0.31522	0.29075	0.26201	0.46560	0.43346
γ_3	0.32302	0.31453	0.29411	0.26763	0.45327	0.43216
γ_4	0.31358	0.30967	0.29322	0.26933	0.43498	0.42365
γ_5	0.29989	0.30005	0.28794	0.26757	0.40978	0.40687
γ_6	0.28071	0.28440	0.27685	0.26093	0.37660	0.38022
γ_7	0.25454	0.26084	0.25763	0.24691	0.33446	0.34216
γ_8	0.21993	0.22738	0.22731	0.22122	0.28284	0.29193
γ_9	0.17604	0.18300	0.18433	0.18119	0.22200	0.23030
γ_{10}	0.12332	0.12851	0.12988	0.12823	0.15310	0.15924
γ_{11}	0.06362	0.06636	0.06719	0.06651	0.07818	0.08144
μ_0	0.00091	-0.00509	-0.00913	-0.01117	0.00272	-0.01307
μ_1	0.00093	-0.00121	-0.00307	-0.00412	0.00282	-0.00485
μ_2	0.00102	0.00053	-0.00032	-0.00095	0.00313	0.00030
μ_3	0.00120	0.00105	0.00031	-0.00047	0.00369	0.00258
μ_4	0.00152	0.00162	0.00101	0.00021	0.00454	0.00471
μ_5	0.00204	0.00241	0.00183	0.00081	0.00573	0.00717
μ_6	0.00286	0.00371	0.00338	0.00227	0.00725	0.01044
μ_7	0.00403	0.00562	0.00581	0.00475	0.00891	0.01417
μ_8	0.00543	0.00803	0.00929	0.00898	0.01026	0.01749
μ_9	0.00652	0.01000	0.01242	0.01337	0.01053	0.01862
μ_{10}	0.00633	0.00981	0.01262	0.01440	0.00892	0.01595
μ_{11}	0.00401	0.00619	0.00799	0.00923	0.00517	0.00920
K_0	0.00119	-0.00105	-0.00053	+0.00133	0.00117	-0.00525
K_1	0.00118	0.00048	-0.00128	-0.00286	0.00120	-0.00288
K_2	0.00115	0.00114	0.00059	+0.00004	0.00132	-0.00028
K_3	0.00112	0.00082	0.00013	-0.00053	0.00157	-0.00039
K_4	0.00112	0.00082	0.00030	-0.00180	0.00206	-0.00012
K_5	0.00123	0.00061	-0.00033	-0.00103	0.00301	-0.00015
K_6	0.00161	0.00079	-0.00048	-0.00137	0.00478	0.00137
K_7	0.00261	0.00155	-0.00062	-0.00258	0.00783	0.00533
K_8	0.00482	0.00438	0.00205	-0.00127	0.01225	0.01374
K_9	0.00844	0.01006	0.00967	0.00702	0.01664	0.02402
K_{10}	0.01137	0.01560	0.01905	0.02060	0.01754	0.02863
K_{11}	0.00892	0.01283	0.01682	0.02003	0.01165	0.01987
C_L	4.59406	4.50133	4.25436	3.92240	3.95659	3.80437
$-C_m$	1.11027	3.15643	5.02487	6.57948	0.93449	2.62785
$\frac{x_{ac}}{\bar{c}}$	0.24168	0.70122	1.18111	1.67741	0.23619	0.69075
$\bar{\eta}$	0.44843	0.45818	0.46761	0.47597	0.43951	0.45235

Table 3 (contd.)/

Table 3 (contd.)

Solutions with $\lambda = 1$, $(m,N,q) = (23,3,4)$, NLR Rounding, $M = 0$, $\alpha = 1$

WING A $A\tan\Lambda_{\frac{1}{2}}$	7 5 4	8 5 6	9 3 0	10 3 2	11 3 4	12 3 6
γ_0	0.35280	0.29066	0.64764	0.55568	0.42561	0.32693
γ_1	0.36462	0.30430	0.64341	0.56353	0.44104	0.34344
γ_2	0.37702	0.31858	0.63062	0.56931	0.45778	0.36061
γ_3	0.38348	0.32813	0.60895	0.56586	0.46809	0.37380
γ_4	0.38337	0.33236	0.57794	0.55116	0.46944	0.38084
γ_5	0.37610	0.33197	0.53710	0.52376	0.46018	0.38297
γ_6	0.35896	0.32396	0.48608	0.48235	0.43563	0.37463
γ_7	0.32912	0.30430	0.42485	0.42685	0.39351	0.34952
γ_8	0.28437	0.26776	0.35386	0.35834	0.33416	0.30275
γ_9	0.22592	0.21480	0.27410	0.27900	0.26191	0.23944
γ_{10}	0.15681	0.14977	0.18711	0.19112	0.18028	0.16564
γ_{11}	0.08043	0.07713	0.09492	0.09719	0.09208	0.08504
μ_0	-0.02112	-0.02252	0.00987	-0.02942	-0.04097	-0.03675
μ_1	-0.00931	-0.01002	0.01008	-0.01404	-0.02125	-0.01748
μ_2	-0.00229	-0.00294	0.01073	-0.00151	-0.00700	-0.00480
μ_3	-0.00006	-0.00160	0.01180	0.00565	-0.00176	-0.00255
μ_4	0.00211	0.00007	0.01324	0.01200	0.00303	-0.00005
μ_5	0.00450	0.00142	0.01493	0.01836	0.00835	0.00155
μ_6	0.00847	0.00460	0.01659	0.02505	0.01668	0.00669
μ_7	0.01378	0.00977	0.01777	0.03072	0.02622	0.01547
μ_8	0.01961	0.01736	0.01785	0.03366	0.03420	0.02692
μ_9	0.02270	0.02288	0.01620	0.03192	0.03570	0.03274
μ_{10}	0.02022	0.02176	0.01245	0.02489	0.02907	0.02874
μ_{11}	0.01173	0.01279	0.00680	0.01356	0.01594	0.01600
κ_0	-0.00055	+0.00623	0.00369	-0.01561	+0.00405	+0.01736
κ_1	-0.00731	-0.00982	0.00388	-0.01462	-0.01816	-0.01820
κ_2	-0.00259	-0.00336	0.00451	-0.00902	-0.01135	-0.00689
κ_3	-0.00239	-0.00290	0.00572	-0.00751	-0.00870	-0.00353
κ_4	-0.00190	-0.00179	0.00775	-0.00572	-0.00841	-0.00166
κ_5	-0.00347	-0.00331	0.01092	-0.00321	-0.01292	-0.00523
κ_6	-0.00411	-0.00514	0.01544	0.00450	-0.01473	-0.01220
κ_7	-0.00278	-0.00830	0.02102	0.01838	-0.00711	-0.01936
κ_8	0.00697	-0.00300	0.02632	0.03703	0.01808	-0.00555
κ_9	0.02413	0.01704	0.02872	0.05111	0.04847	0.03093
κ_{10}	0.03600	0.03724	0.02532	0.05059	0.06007	0.05635
κ_{11}	0.02690	0.03077	0.01502	0.03145	0.04050	0.04235
C_L	3.43042	2.99544	3.14557	2.94611	2.48965	2.04669
$-C_m$	4.03037	5.03187	0.70684	1.99847	2.91613	3.44584
$\frac{x_{ac}}{\bar{c}}$	1.17489	1.67985	0.22471	0.67834	1.17130	1.68362
$\bar{\eta}$	0.46536	0.47663	0.43205	0.44640	0.46351	0.47754

Table 3 (contd.)/

Table 3 (contd)

Solutions with λ = 1, (m,N,q) = (23,3,4), NLR Rounding, M = 0, α = 1

η	WING A $A\tan\Lambda_{\frac{1}{2}}$	13 1.5 0	14 1.5 2	15 1.5 4	16 1.5 6
0	γ_0	0.85103	0.71788	0.48431	0.35029
0.13053	γ_1	0.84423	0.72734	0.50442	0.36903
0.25882	γ_2	0.82388	0.73115	0.52616	0.38739
0.38268	γ_3	0.79010	0.72088	0.54170	0.40294
0.50000	γ_4	0.74314	0.69381	0.54594	0.41250
0.60876	γ_5	0.68346	0.64940	0.53470	0.41838
0.70711	γ_6	0.61170	0.58826	0.50111	0.41116
0.79335	γ_7	0.52882	0.51278	0.44584	0.38121
0.86603	γ_8	0.43604	0.42538	0.37340	0.32592
0.92388	γ_9	0.33486	0.32845	0.29027	0.25544
0.96593	γ_{10}	0.22707	0.22376	0.19899	0.17604
0.99144	γ_{11}	0.11470	0.11343	0.10146	0.09030
	μ_0	0.03892	-0.06626	-0.06923	-0.05119
	μ_1	0.03908	-0.03882	-0.04136	-0.02520
	μ_2	0.03954	-0.01050	-0.01706	-0.00593
	μ_3	0.04013	0.00937	-0.00731	-0.00307
	μ_4	0.04060	0.02658	0.00140	-0.00057
	μ_5	0.04060	0.04136	0.01175	-0.00002
	μ_6	0.03969	0.05327	0.02706	0.00691
	μ_7	0.03742	0.05984	0.04185	0.02033
	μ_8	0.03339	0.05955	0.05120	0.03566
	μ_9	0.02739	0.05166	0.04960	0.04117
	μ_{10}	0.01951	0.03769	0.03791	0.03427
	μ_{11}	0.01016	0.01974	0.02002	0.01842
	K_0	0.02551	-0.04408	+0.02434	+0.03415
	K_1	0.02630	-0.05658	-0.03181	-0.02753
	K_2	0.02868	-0.05529	-0.03158	-0.01103
	K_3	0.03260	-0.05045	-0.02354	-0.00212
	K_4	0.03789	-0.03922	-0.02450	+0.00072
	K_5	0.04403	-0.01963	-0.03551	-0.00633
	K_6	0.04999	0.01309	-0.03835	-0.02377
	K_7	0.05416	0.05297	-0.01506	-0.03604
	K_8	0.05455	0.08802	0.03563	-0.00910
	K_9	0.04936	0.10225	0.08141	0.04543
	K_{10}	0.03777	0.08918	0.08941	0.07420
	K_{11}	0.02054	0.05156	0.05656	0.05273
	C_L	2.02179	1.84867	1.42795	1.10643
	$-C_m$	0.39343	1.23008	1.67641	1.86864
	$\frac{x_{ac}}{c}$	0.19460	0.66539	1.17400	1.68890
	$\bar{\eta}$	0.42650	0.43895	0.46237	0.47857

Table 4/

Table 4

Solutions with λ = 0.5, (m,N,q) = (23,3,4), NLR Rounding, M = 0, α = 1

WING A $A\tan\Lambda_{\frac{1}{2}}$	17 8 0	18 8 2	19 8 4	20 8 6	21 5 0	22 5 2
γ_0	0.37894	0.35204	0.31800	0.28315	0.52165	0.47076
γ_1	0.37308	0.35153	0.32151	0.28913	0.51469	0.47112
γ_2	0.35933	0.34489	0.31991	0.29043	0.49764	0.46512
γ_3	0.34066	0.33194	0.31138	0.28478	0.47325	0.45105
γ_4	0.31851	0.31448	0.29793	0.27415	0.44278	0.42995
γ_5	0.29372	0.29362	0.28111	0.26062	0.40707	0.40256
γ_6	0.26642	0.26968	0.26126	0.24452	0.36636	0.36888
γ_7	0.23606	0.24202	0.23778	0.22560	0.32038	0.32805
γ_8	0.20136	0.20896	0.20834	0.20099	0.26843	0.27867
γ_9	0.16067	0.16830	0.16984	0.16638	0.20984	0.21988
γ_{10}	0.11286	0.11881	0.12066	0.11913	0.14465	0.15234
γ_{11}	0.05847	0.06167	0.06281	0.06224	0.07393	0.07808
μ_0	0.00071	-0.00698	-0.01232	-0.01514	0.00199	-0.01719
μ_1	0.00144	-0.00210	-0.00489	-0.00644	0.00350	-0.00773
μ_2	0.00160	0.00027	-0.00111	-0.00197	0.00431	-0.00141
μ_3	0.00151	0.00080	-0.00026	-0.00114	0.00445	0.00103
μ_4	0.00149	0.00112	0.00030	-0.00047	0.00461	0.00262
μ_5	0.00161	0.00146	0.00070	-0.00017	0.00499	0.00410
μ_6	0.00194	0.00209	0.00147	0.00057	0.00573	0.00612
μ_7	0.00256	0.00314	0.00273	0.00168	0.00682	0.00886
μ_8	0.00354	0.00485	0.00506	0.00423	0.00811	0.01217
μ_9	0.00469	0.00694	0.00819	0.00820	0.00895	0.01472
μ_{10}	0.00518	0.00796	0.01008	0.01125	0.00826	0.01416
μ_{11}	0.00365	0.00562	0.00724	0.00834	0.00510	0.00880
κ_0	-0.00229	-0.00486	-0.00355	-0.00036	-0.00816	-0.01402
κ_1	0.00065	-0.00066	-0.00270	-0.00455	-0.00110	-0.00610
κ_2	0.00117	0.00091	+0.00004	-0.00087	0.00149	-0.00101
κ_3	0.00108	0.00064	-0.00023	-0.00111	0.00169	-0.00070
κ_4	0.00108	0.00076	+0.00023	-0.00033	0.00192	-0.00029
κ_5	0.00111	0.00053	-0.00027	-0.00096	0.00239	-0.00070
κ_6	0.00126	0.00061	-0.00022	-0.00082	0.00340	-0.00030
κ_7	0.00168	0.00065	-0.00085	-0.00190	0.00536	0.00087
κ_8	0.00283	0.00018	-0.00039	-0.00240	0.00886	0.00575
κ_9	0.00545	0.00522	0.00311	-0.00016	0.01371	0.01518
κ_{10}	0.00904	0.01144	0.01251	0.01174	0.01682	0.02421
κ_{11}	0.00851	0.01187	0.01502	0.01732	0.01249	0.01973
C_L	4.73571	4.63981	4.38473	4.04096	4.07246	3.91891
$-C_m$	1.88838	3.91742	5.72781	7.18844	1.59988	3.31242
$\frac{x_{ac}}{\bar{c}}$	0.39875	0.84431	1.30631	1.77889	0.39285	0.84524
$\bar{\eta}$	0.42876	0.43798	0.44610	0.45261	0.42635	0.43821

Table 4 (contd.)/

Table 4 (contd)

Solutions with $\lambda = 0.5$, $(m,N,q) = (23,3,4)$, NLR Rounding, $M = 0$, $\alpha = 1$

WING A $A\tan\Lambda_{\frac{1}{2}}$	23 5 4	24 5 6	25 3 0	26 3 2	27 3 4	28 3 6
γ_0	0.40204	0.33784	0.68768	0.60307	0.47841	0.37840
γ_1	0.40787	0.34640	0.67957	0.60428	0.48698	0.38934
γ_2	0.40916	0.35069	0.65864	0.59854	0.49127	0.39585
γ_3	0.40242	0.34752	0.62735	0.58290	0.48693	0.39500
γ_4	0.38878	0.33793	0.58678	0.55739	0.47417	0.38681
γ_5	0.36972	0.32450	0.53778	0.52200	0.45401	0.37454
γ_6	0.34486	0.30690	0.48086	0.47621	0.42456	0.35699
γ_7	0.31285	0.28424	0.41638	0.41943	0.38320	0.33199
γ_8	0.27047	0.25139	0.34459	0.35152	0.32682	0.29137
γ_9	0.21596	0.20408	0.26592	0.27358	0.25684	0.23275
γ_{10}	0.15048	0.14319	0.18121	0.18748	0.17697	0.16131
γ_{11}	0.07743	0.07403	0.09187	0.09542	0.09054	0.08301
μ_0	-0.02713	-0.02919	0.00708	-0.03802	-0.05072	-0.04618
μ_1	-0.01366	-0.01443	0.00973	-0.02176	-0.02989	-0.02483
μ_2	-0.00486	-0.00517	0.01193	-0.00795	-0.01320	-0.00898
μ_3	-0.00200	-0.00306	0.01298	-0.00055	-0.00644	-0.00490
μ_4	-0.00016	-0.00150	0.01375	0.00487	-0.00209	-0.00225
μ_5	0.00125	-0.00079	0.01456	0.00977	0.00125	-0.00133
μ_6	0.00351	0.00088	0.01557	0.01522	0.00634	0.00112
μ_7	0.00687	0.00344	0.01658	0.02098	0.01351	0.00526
μ_8	0.01194	0.00887	0.01711	0.02593	0.02251	0.01438
μ_9	0.01677	0.01552	0.01626	0.02754	0.02848	0.02366
μ_{10}	0.01751	0.01835	0.01313	0.02343	0.02656	0.02547
μ_{11}	0.01109	0.01199	0.00742	0.01340	0.01550	0.01538
κ_0	-0.00577	+0.00420	-0.02167	-0.03181	-0.00086	+0.01649
κ_1	-0.00890	-0.01058	-0.00687	-0.02157	-0.01720	-0.01664
κ_2	-0.00323	-0.00406	0.00229	-0.01145	-0.01173	-0.00852
κ_3	-0.00256	-0.00323	0.00528	-0.00887	-0.00819	-0.00396
κ_4	-0.00144	-0.00165	0.00728	-0.00741	-0.00553	-0.00061
κ_5	-0.00265	-0.00276	0.00967	-0.00756	-0.00841	-0.00207
κ_6	-0.00322	-0.00296	0.01340	-0.00514	-0.01216	-0.00387
κ_7	-0.00492	-0.00602	0.01876	0.00182	-0.01623	-0.01224
κ_8	-0.00231	-0.00777	0.02529	0.01752	-0.00680	-0.01757
κ_9	0.00930	0.00037	0.03041	0.03701	0.02091	0.00119
κ_{10}	0.02660	0.02371	0.02938	0.04638	0.04714	0.03818
κ_{11}	0.02516	0.02763	0.01854	0.03234	0.03853	0.03874
C_L	3.53909	3.09293	3.21594	3.02194	2.56829	2.11783
$-C_m$	4.66260	5.56344	1.22414	2.56112	3.41877	3.84507
$\frac{x_{ac}}{\bar{c}}$	1.31746	1.79876	0.38065	0.84751	1.33115	1.81557
$\bar{\eta}$	0.44875	0.45674	0.42438	0.43736	0.45058	0.45980

Table 4 (contd.)

Table 4 (contd.)

Solutions with λ = 0.5, (m,N,q) = (23,3,4), NLR Rounding, M = 0, α = 1

η	WING A $A\tan\Lambda_{\frac{1}{2}}$	29 1.5 0	30 1.5 2	31 1.5 4	32 1.5 6
0	γ_0	0.87204	0.75574	0.54031	0.40477
0.13053	γ_1	0.86328	0.75806	0.55287	0.41798
0.25882	γ_2	0.83855	0.75139	0.56048	0.42579
0.38268	γ_3	0.79960	0.73176	0.55907	0.42635
0.50000	γ_4	0.74757	0.69827	0.54846	0.41917
0.60876	γ_5	0.68358	0.65039	0.52861	0.40833
0.70711	γ_6	0.60865	0.58790	0.49479	0.39222
0.79335	γ_7	0.52392	0.51183	0.44300	0.36655
0.86603	γ_8	0.43054	0.42411	0.37253	0.31931
0.92388	γ_9	0.32984	0.32717	0.28934	0.25181
0.96593	γ_{10}	0.22330	0.22286	0.19816	0.17332
0.99144	γ_{11}	0.11270	0.11302	0.10115	0.08904
	μ_0	0.02882	-0.08209	-0.08253	-0.06257
	μ_1	0.03280	-0.05588	-0.05521	-0.03598
	μ_2	0.03701	-0.02846	-0.02846	-0.01274
	μ_3	0.03964	-0.00959	-0.01577	-0.00610
	μ_4	0.04128	0.00590	-0.00781	-0.00242
	μ_5	0.04206	0.01965	-0.00163	-0.00181
	μ_6	0.04196	0.03253	0.00826	0.00050
	μ_7	0.04059	0.04299	0.02171	0.00574
	μ_8	0.03738	0.04875	0.03559	0.01904
	μ_9	0.03168	0.04686	0.04172	0.03097
	μ_{10}	0.02322	0.03647	0.03592	0.03140
	μ_{11}	0.01232	0.01972	0.01985	0.01803
	K_0	-0.05094	-0.05746	+0.02817	+0.03855
	K_1	-0.02178	-0.05623	-0.01838	-0.02085
	K_2	0.00582	-0.05072	-0.02750	-0.01603
	K_3	0.02268	-0.04963	-0.02111	-0.00428
	K_4	0.03536	-0.04771	-0.01542	0.00223
	K_5	0.04645	-0.04396	-0.02179	0.00156
	K_6	0.05708	-0.02910	-0.03424	-0.00241
	K_7	0.06623	0.00050	-0.04117	-0.02032
	K_8	0.07126	0.04277	-0.01569	-0.03299
	K_9	0.06842	0.07743	0.03686	0.00140
	K_{10}	0.05483	0.08242	0.07176	0.05207
	K_{11}	0.03069	0.05206	0.05369	0.04868
	C_L	2.03956	1.88063	1.47324	1.14743
	$-C_m$	0.71419	1.60883	1.98939	2.09896
	$\frac{x_{ac}}{\bar{c}}$	0.35017	0.85548	1.35035	1.82926
	$\bar{\eta}$	0.42325	0.43437	0.45196	0.46191

Table 5/

Table 5

Solutions with $\lambda = 0.25$, $(m,N,q) = (23,3,4)$, NLR Rounding, $M = 0$, $\alpha = 1$

WING A $A\tan\Lambda_{\frac{1}{2}}$	33 8 0	34 8 2	35 8 4	36 8 6	37 5 0	38 5 2
γ_0	0.40653	0.38046	0.34672	0.31140	0.54709	0.49933
γ_1	0.39803	0.37684	0.34705	0.31447	0.53764	0.49614
γ_2	0.37805	0.36373	0.33912	0.30986	0.51475	0.48313
γ_3	0.35092	0.34234	0.32228	0.29625	0.48246	0.46029
γ_4	0.31915	0.31524	0.29922	0.27622	0.44294	0.42947
γ_5	0.28481	0.28464	0.27243	0.25270	0.39826	0.39257
γ_6	0.24937	0.25221	0.24358	0.22717	0.35007	0.35115
γ_7	0.21366	0.21891	0.21386	0.20117	0.29947	0.30606
γ_8	0.17760	0.18456	0.18293	0.17435	0.24668	0.25690
γ_9	0.13991	0.14748	0.14865	0.14439	0.19102	0.20216
γ_{10}	0.09833	0.10470	0.10685	0.10537	0.13135	0.14044
γ_{11}	0.05128	0.05484	0.05626	0.05584	0.06723	0.07226
μ_0	0.00056	-0.00832	-0.01460	-0.01804	0.00123	-0.02009
μ_1	0.00188	-0.00275	-0.00628	-0.00824	0.00374	-0.00986
μ_2	0.00220	0.00014	-0.00173	-0.00281	0.00512	-0.00269
μ_3	0.00190	0.00070	-0.00066	-0.00166	0.00508	-0.00005
μ_4	0.00162	0.00088	-0.00013	-0.00093	0.00473	0.00122
μ_5	0.00144	0.00095	0.00009	-0.00070	0.00441	0.00200
μ_6	0.00141	0.00114	0.00045	-0.00024	0.00437	0.00294
μ_7	0.00155	0.00151	0.00091	0.00012	0.00468	0.00434
μ_8	0.00197	0.00231	0.00194	0.00115	0.00543	0.00655
μ_9	0.00275	0.00375	0.00392	0.00329	0.00640	0.00937
μ_{10}	0.00360	0.00539	0.00659	0.00697	0.00671	0.01096
μ_{11}	0.00305	0.00471	0.00606	0.00694	0.00467	0.00789
K_0	-0.00603	-0.00876	-0.00672	-0.00242	-0.01793	-0.02251
K_1	-0.00030	-0.00202	-0.00390	-0.00552	-0.00508	-0.00992
K_2	0.00103	0.00056	-0.00039	-0.00138	0.00040	-0.00227
K_3	0.00093	0.00037	-0.00057	-0.00156	0.00098	-0.00131
K_4	0.00093	0.00059	+0.00008	-0.00054	0.00110	-0.00063
K_5	0.00094	0.00041	-0.00029	-0.00097	0.00126	-0.00100
K_6	0.00100	0.00056	+0.00006	-0.00037	0.00171	-0.00082
K_7	0.00111	0.00041	-0.00043	-0.00097	0.00261	-0.00101
K_8	0.00146	0.00064	-0.00048	-0.00122	0.00445	0.00038
K_9	0.00259	0.00159	-0.00043	-0.00242	0.00807	0.00515
K_{10}	0.00542	0.00592	0.00495	0.00271	0.01267	0.01534
K_{11}	0.00707	0.00958	0.01163	0.01281	0.01173	0.01750
C_L	4.75529	4.65978	4.40618	4.06367	4.08162	3.93101
$-C_m$	2.46503	4.43334	6.15546	7.50961	2.10001	3.78751
$\frac{x_{ac}}{\bar{c}}$	0.51838	0.95141	1.39701	1.84799	0.51450	0.96349
$\bar{\eta}$	0.41214	0.42071	0.42751	0.43232	0.41516	0.42600

Table 5 (contd.)/

Solutions with λ = 0.25, (m,N,q) = (23,3,4), NLR Rounding, M = 0, α = 1

WING A $A\tan\Lambda_{\frac{1}{2}}$	39 5 4	40 5 6	41 3 0	42 3 2	43 3 4	44 3 6
y_0	0.43305	0.36925	0.70568	0.62860	0.51109	0.41256
y_1	0.43512	0.37445	0.69564	0.62583	0.51532	0.41992
y_2	0.42920	0.37211	0.67005	0.61282	0.51154	0.41932
y_3	0.41322	0.35999	0.63260	0.58867	0.49694	0.40857
y_4	0.38910	0.33982	0.58513	0.55447	0.47290	0.38876
y_5	0.35934	0.31501	0.52947	0.51145	0.44176	0.36377
y_6	0.32543	0.28684	0.46714	0.46054	0.40441	0.33461
y_7	0.28840	0.25720	0.39947	0.40208	0.36105	0.30336
y_8	0.24697	0.22460	0.32725	0.33569	0.30867	0.26666
y_9	0.19814	0.18472	0.25085	0.26112	0.24442	0.21750
y_{10}	0.13919	0.13167	0.17036	0.17910	0.16903	0.15231
y_{11}	0.07204	0.06859	0.08629	0.09129	0.08673	0.07865
μ_0	-0.03132	-0.03394	0.00418	-0.04372	-0.05726	-0.05280
μ_1	-0.01693	-0.01792	0.00826	-0.02704	-0.03602	-0.03066
μ_2	-0.00689	-0.00711	0.01162	-0.01253	-0.01792	-0.01271
μ_3	-0.00344	-0.00425	0.01280	-0.00498	-0.00991	-0.00697
μ_4	-0.00166	-0.00266	0.01305	-0.00028	-0.00540	-0.00401
μ_5	-0.00076	-0.00222	0.01295	0.00318	-0.00290	-0.00329
μ_6	0.00038	-0.00130	0.01300	0.00669	-0.00015	-0.00196
μ_7	0.00189	-0.00042	0.01333	0.01083	0.00349	-0.00071
μ_8	0.00484	0.00213	0.01387	0.01571	0.00988	0.00367
μ_9	0.00928	0.00699	0.01396	0.01988	0.01761	0.01185
μ_{10}	0.01293	0.01271	0.01227	0.01991	0.02139	0.01901
μ_{11}	0.00986	0.01057	0.00745	0.01261	0.01439	0.01406
K_0	-0.01091	+0.00173	-0.04684	-0.04567	-0.00495	+0.01598
K_1	-0.01038	-0.01063	-0.02158	-0.02838	-0.01603	-0.01404
K_2	-0.00363	-0.00421	-0.00490	-0.01378	-0.01067	-0.00871
K_3	-0.00262	-0.00332	0.00048	-0.00937	-0.00691	-0.00381
K_4	-0.00114	-0.00167	0.00277	-0.00703	-0.00286	+0.00010
K_5	-0.00208	-0.00294	0.00445	-0.00741	-0.00375	-0.00134
K_6	-0.00194	-0.00245	0.00676	-0.00735	-0.00478	-0.00126
K_7	-0.00358	-0.00398	0.01046	-0.00689	-0.01011	-0.00457
K_8	-0.00423	-0.00541	0.01610	-0.00050	-0.01351	-0.01017
K_9	-0.00199	-0.00734	0.02315	0.01499	-0.00503	-0.01423
K_{10}	0.01263	0.00663	0.02689	0.03376	0.02521	0.01208
K_{11}	0.02101	0.02184	0.01942	0.03032	0.03352	0.03169
C_L	3.55619	3.11216	3.21186	3.02612	2.58270	2.13464
$-C_m$	5.06202	5.85861	1.62337	2.96415	3.74968	4.07814
$\frac{x_{ac}}{\bar{c}}$	1.42344	1.88249	0.50543	0.97952	1.45185	1.91046
$\bar{\eta}$	0.43419	0.43914	0.41782	0.42954	0.43915	0.44393

Table 5 (contd.)/

Table 5 (contd.)

Solutions with λ = 0.25, (m,N,q) = (23,3,4), NLR Rounding, M = 0, α = 1

η	WING A $A\tan\Lambda_{\frac{1}{2}}$	45 1.5 0	46 1.5 2	47 1.5 4	48 1.5 6
	γ_0	0.87630	0.77472	0.57544	0.44163
0.13053	γ_1	0.86704	0.77255	0.58310	0.45147
0.25882	γ_2	0.84005	0.75896	0.58170	0.45200
0.38268	γ_3	0.79787	0.73232	0.56857	0.44198
0.50000	γ_4	0.74227	0.69306	0.54522	0.42242
0.60876	γ_5	0.67502	0.64154	0.51401	0.39748
0.70711	γ_6	0.59760	0.57795	0.47483	0.36814
0.79335	γ_7	0.51161	0.50259	0.42593	0.33681
0.86603	γ_8	0.41840	0.41626	0.36203	0.29775
0.92388	γ_9	0.31933	0.32088	0.28272	0.24076
0.96593	γ_{10}	0.21560	0.21855	0.19345	0.16641
0.99144	γ_{11}	0.10864	0.11091	0.09888	0.08560
	μ_0	0.01767	-0.09158	-0.09133	-0.07093
	μ_1	0.02336	-0.06633	-0.06457	-0.04457
	μ_2	0.02941	-0.04001	-0.03693	-0.01880
	μ_3	0.03303	-0.02251	-0.02201	-0.00911
	μ_4	0.03510	-0.00931	-0.01302	-0.00438
	μ_5	0.03606	0.00167	-0.00801	-0.00330
	μ_6	0.03632	0.01229	-0.00290	-0.00178
	μ_7	0.03589	0.02276	0.00419	-0.00073
	μ_8	0.03439	0.03200	0.01600	0.00508
	μ_9	0.03079	0.03676	0.02769	0.01649
	μ_{10}	0.02388	0.03287	0.03079	0.02454
	μ_{11}	0.01320	0.01909	0.01900	0.01683
	K_0	-0.12616	-0.06316	+0.03255	+0.04372
	K_1	-0.07844	-0.05216	-0.00611	-0.01283
	K_2	-0.03404	-0.04015	-0.01942	-0.01676
	K_3	-0.00862	-0.03681	-0.01685	-0.00501
	K_4	0.00802	-0.03597	-0.00830	0.00335
	K_5	0.02095	-0.03902	-0.00677	0.00343
	K_6	0.03327	-0.03965	-0.01015	0.00375
	K_7	0.04609	-0.03287	-0.02430	-0.00092
	K_8	0.05798	-0.00736	-0.03448	-0.01385
	K_9	0.06439	0.03380	-0.01235	-0.02272
	K_{10}	0.05790	0.06408	0.04074	0.01726
	K_{11}	0.03486	0.04951	0.04761	0.04046
	C_L	2.02636	1.88054	1.48448	1.16048
	$-C_m$	0.97842	1.89138	2.20314	2.24131
	$\frac{x_{ac}}{\bar{c}}$	0.48284	1.00577	1.48412	1.93137
	$\bar{\eta}$	0.42039	0.43047	0.44270	0.44696

Table 6/

Table 6

Solutions with λ = 0, (m,N,q) = (23,3,4), NLR Rounding, M = 0, α = 1

WING A $A\tan\Lambda_{\frac{1}{2}}$	49 8 0	50 8 2	51 8 4	52 8 6	53 5 0	54 5 2
γ_0	0.43515	0.41187	0.38054	0.34645	0.56633	0.52622
γ_1	0.42382	0.40468	0.37707	0.34588	0.55432	0.51896
γ_2	0.39658	0.38375	0.36129	0.33384	0.52462	0.49739
γ_3	0.35860	0.35135	0.33356	0.30976	0.48201	0.46284
γ_4	0.31292	0.31031	0.29672	0.27645	0.42897	0.41733
γ_5	0.26261	0.26356	0.25383	0.23731	0.36832	0.36325
γ_6	0.21047	0.21388	0.20750	0.19462	0.30289	0.30328
γ_7	0.15916	0.16397	0.16046	0.15120	0.23591	0.24035
γ_8	0.11109	0.11624	0.11487	0.10876	0.17052	0.17743
γ_9	0.06858	0.07315	0.07320	0.06970	0.11016	0.11781
γ_{10}	0.03380	0.03700	0.03766	0.03614	0.05815	0.06462
γ_{11}	0.00948	0.01085	0.01150	0.01143	0.01903	0.02252
μ_0	0.00049	-0.00987	-0.01745	-0.02185	0.00051	-0.02302
μ_1	0.00263	-0.00344	-0.00808	-0.01072	0.00420	-0.01201
μ_2	0.00333	0.00019	-0.00248	-0.00401	0.00647	-0.00379
μ_3	0.00280	0.00088	-0.00103	-0.00235	0.00638	-0.00073
μ_4	0.00216	0.00092	-0.00046	-0.00145	0.00544	0.00034
μ_5	0.00161	0.00079	-0.00023	-0.00100	0.00422	0.00049
μ_6	0.00124	0.00076	0.00016	-0.00018	0.00313	0.00041
μ_7	0.00098	0.00077	0.00050	0.00045	0.00222	0.00032
μ_8	0.00079	0.00083	0.00089	0.00113	0.00158	0.00049
μ_9	0.00053	0.00069	0.00089	0.00114	0.00112	0.00080
μ_{10}	0.00017	0.00034	0.00057	0.00081	0.00074	0.00099
μ_{11}	-0.00017	-0.00016	-0.00011	-0.00005	0.00006	0.00026
κ_0	-0.01292	-0.01579	-0.01258	-0.00655	-0.03475	-0.03709
κ_1	-0.00269	-0.00490	-0.00614	-0.00685	-0.01369	-0.01763
κ_2	0.00045	-0.00038	-0.00119	-0.00195	-0.00302	-0.00559
κ_3	0.00049	-0.00031	-0.00126	-0.00225	-0.00114	-0.00316
κ_4	0.00057	0.00008	-0.00043	-0.00104	-0.00078	-0.00189
κ_5	0.00070	0.00012	-0.00050	-0.00097	-0.00063	-0.00204
κ_6	0.00089	0.00073	0.00075	0.00110	-0.00039	-0.00151
κ_7	0.00098	0.00102	0.00148	0.00260	-0.00003	-0.00145
κ_8	0.00085	0.00144	0.00268	0.00455	0.00041	-0.00002
κ_9	0.00024	0.00092	0.00236	0.00443	0.00076	0.00120
κ_{10}	-0.00081	-0.00038	0.00053	0.00167	0.00057	0.00224
κ_{11}	-0.00110	-0.00122	-0.00123	-0.00118	-0.00090	-0.00050
C_L	4.54267	4.45775	4.23217	3.92496	3.86317	3.73001
$-C_m$	3.09153	4.81826	6.29637	7.43307	2.63643	4.14269
$\frac{x_{ac}}{c}$	0.68055	1.08087	1.48774	1.89380	0.68245	1.11064
$\bar{\eta}$	0.37437	0.38135	0.38603	0.38869	0.38570	0.39386

Table 6 (contd.)/

Solutions with $\lambda = 0$, (m,N,q) = (23,3,4), NLR Rounding, M = 0, α = 1

WING A $A\tan\Lambda_{\frac{1}{2}}$	55 5 4	56 5 6	57 3 0	58 3 2	59 3 4	60 3 6
γ_0	0.46756	0.40758	0.70817	0.64676	0.54640	0.45431
γ_1	0.46506	0.40857	0.69637	0.63936	0.54520	0.45713
γ_2	0.45016	0.39789	0.66530	0.61719	0.53122	0.44743
γ_3	0.42197	0.37402	0.61936	0.58107	0.50296	0.42361
γ_4	0.38252	0.33894	0.56077	0.53239	0.46194	0.38722
γ_5	0.33455	0.29620	0.49195	0.47294	0.41054	0.34196
γ_6	0.28056	0.24794	0.41526	0.40492	0.35096	0.28972
γ_7	0.22364	0.19761	0.33378	0.33090	0.28636	0.23462
γ_8	0.16629	0.14694	0.25074	0.25383	0.21930	0.17840
γ_9	0.11166	0.09874	0.17025	0.17728	0.15354	0.12378
γ_{10}	0.06209	0.05474	0.09655	0.10488	0.09108	0.07252
γ_{11}	0.02215	0.01960	0.03635	0.04208	0.03599	0.02730
μ_0	-0.03618	-0.03999	0.00089	-0.04833	-0.06435	-0.06117
μ_1	-0.02089	-0.02274	0.00630	-0.03145	-0.04289	-0.03855
μ_2	-0.00937	-0.00999	0.01094	-0.01631	-0.02342	-0.01822
μ_3	-0.00499	-0.00595	0.01234	-0.00851	-0.01372	-0.01008
μ_4	-0.00306	-0.00419	0.01190	-0.00434	-0.00848	-0.00657
μ_5	-0.00244	-0.00383	0.01035	-0.00231	-0.00629	-0.00636
μ_6	-0.00193	-0.00290	0.00839	-0.00142	-0.00533	-0.00609
μ_7	-0.00141	-0.00183	0.00630	-0.00123	-0.00515	-0.00553
μ_8	-0.00027	0.00014	0.00441	-0.00120	-0.00380	-0.00227
μ_9	0.00078	0.00132	0.00280	-0.00066	-0.00123	0.00087
μ_{10}	0.00134	0.00164	0.00177	0.00093	0.00168	0.00220
μ_{11}	0.00053	0.00078	0.00079	0.00120	0.00158	0.00206
K_0	-0.02009	-0.00294	-0.08674	-0.06903	-0.01301	+0.01492
K_1	-0.01367	-0.01071	-0.04812	-0.04180	-0.01592	-0.00967
K_2	-0.00462	-0.00402	-0.02052	-0.01986	-0.00891	-0.00712
K_3	-0.00296	-0.00319	-0.01053	-0.01177	-0.00480	-0.00255
K_4	-0.00135	-0.00204	-0.00678	-0.00703	+0.00024	+0.00119
K_5	-0.00266	-0.00436	-0.00511	-0.00537	-0.00034	-0.00307
K_6	-0.00217	-0.00345	-0.00410	-0.00382	-0.00105	-0.00640
K_7	-0.00227	-0.00193	-0.00312	-0.00453	-0.00539	-0.00813
K_8	0.00072	0.00289	-0.00232	-0.00425	-0.00477	-0.00255
K_9	0.00346	0.00715	-0.00126	-0.00351	-0.00027	0.00554
K_{10}	0.00538	0.00892	0.00033	0.00240	0.00842	0.01513
K_{11}	0.00024	0.00056	0.00051	0.00409	0.00803	0.00740
C_L	3.39761	2.99874	3.02563	2.86019	2.46336	2.05552
$-C_m$	5.21826	5.84144	2.06637	3.28584	3.90560	4.09201
$\frac{x_{ac}}{\bar{c}}$	1.53586	1.94797	0.68295	1.14882	1.58547	1.99075
$\bar{\eta}$	0.39775	0.39855	0.39717	0.40504	0.40680	0.40479

Table 6 (contd.)/

Table 6 (contd)

Solutions with $\lambda = 0$, $(m,N,q) = (23,3,4)$, NLR Rounding, $M = 0$, $\alpha = 1$

η	WING A $A\tan\Lambda_{\frac{1}{2}}$	61 1.5 0	62 1.5 2	63 1.5 4	64 1.5 6
0	y_0	0.85944	0.78187	0.61487	0.48759
0.13053	y_1	0.85034	0.77410	0.61605	0.49286
0.25882	y_2	0.82073	0.75095	0.60328	0.48386
0.38268	y_3	0.77355	0.71295	0.57478	0.45953
0.50000	y_4	0.71120	0.66113	0.53218	0.42154
0.60876	y_5	0.63618	0.59678	0.47778	0.37382
0.70711	y_6	0.55045	0.52164	0.41351	0.31830
0.79335	y_7	0.45671	0.43772	0.34278	0.25986
0.86603	y_8	0.35746	0.34750	0.26798	0.20019
0.92388	y_9	0.25646	0.25403	0.19367	0.14205
0.96593	y_{10}	0.15755	0.16085	0.11993	0.08630
0.99144	y_{11}	0.06810	0.07319	0.05159	0.03435
	μ_0	0.00336	-0.09719	-0.10103	-0.08192
	μ_1	0.01011	-0.07324	-0.07493	-0.05606
	μ_2	0.01729	-0.04848	-0.04688	-0.02775
	μ_3	0.02111	-0.03274	-0.02929	-0.01387
	μ_4	0.02245	-0.02236	-0.01773	-0.00741
	μ_5	0.02169	-0.01546	-0.01167	-0.00699
	μ_6	0.01954	-0.01056	-0.00905	-0.00797
	μ_7	0.01636	-0.00760	-0.00969	-0.00965
	μ_8	0.01274	-0.00660	-0.00976	-0.00541
	μ_9	0.00878	-0.00634	-0.00587	0.00002
	μ_{10}	0.00500	-0.00255	0.00172	0.00319
	μ_{11}	0.00250	0.00194	0.00165	0.00259
	K_0	-0.23332	-0.07866	0.03682	0.05082
	K_1	-0.16320	-0.05385	0.00932	0.00012
	K_2	-0.09863	-0.02991	-0.00561	-0.01240
	K_3	-0.06329	-0.01896	-0.00788	-0.00408
	K_4	-0.04357	-0.01214	0.00138	0.00590
	K_5	-0.03196	-0.00848	0.00648	0.00391
	K_6	-0.02464	-0.00288	0.00933	-0.00405
	K_7	-0.01879	-0.00030	0.00088	-0.01431
	K_8	-0.01417	-0.00138	-0.00926	-0.00869
	K_9	-0.01017	-0.01036	-0.00694	0.00211
	K_{10}	-0.00716	-0.00482	0.00567	0.01514
	K_{11}	-0.00027	0.01201	0.02536	0.02006
	C_L	1.92213	1.78519	1.42111	1.11940
	$-C_m$	1.31022	2.15043	2.32504	2.26298
	$\frac{x_{ac}}{\bar{c}}$	0.68165	1.20460	1.63607	2.02160
	$\bar{\eta}$	0.40918	0.41470	0.41315	0.40806

Table 7/

Table 7

Estimated Errors in Lift Slope and Aerodynamic Centre from Data Sheets

Error in $\partial C_L/\partial\alpha$	Number of wings with $A \tan \Lambda_{\frac{1}{2}}$ =			
	0	2	4	6
2 to 4%	2	1	1	0
0 to 2%	7	2	0	1
-2 to 0%	6	6	6	4
-4 to -2%	1	5	2	2
-6 to -4%	0	2	4	2
-8 to -6%	0	0	2	4
-10 to -8%	0	0	1	3

Error in $\bar{x}/\bar{c}$	Number of wings with $A \tan \Lambda_{\frac{1}{2}}$ =		
	0	2	4
0·02 to 0·03	0	0	2
0·01 to 0·02	6	2	3
0 to 0·01	8	6	2
-0·01 to 0	2	4	0
-0·02 to -0·01	0	4	3
-0·03 to -0·02	0	0	6

Table 8/

Table 8

Estimated Errors in Spanwise Centre of Pressure from Ref. 8

Error in $\bar{\eta}$	Number of wings ($\lambda \neq 0$) with $A \tan \Lambda_{\frac{1}{2}} =$			
	0	2	4	6
0·006 to 0·012	0	0	0	3
0·002 to 0·006	0	0	3	5
-0·002 to 0·002	11	11	6	2
-0·006 to -0·002	1	1	2	1
-0·012 to -0·006	0	0	1	1

BMG
BW

FIG. 1

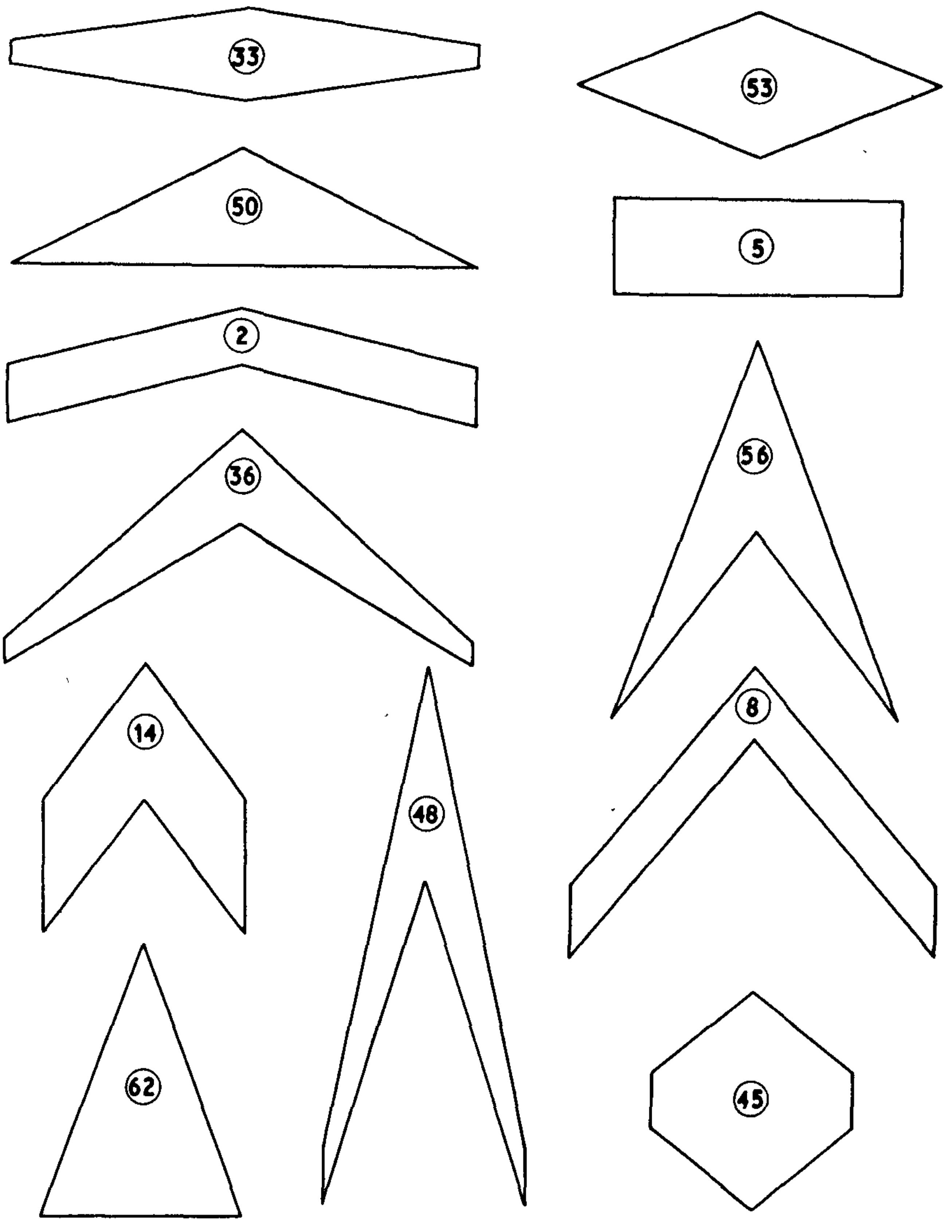

Range of wing planforms

FIG.2

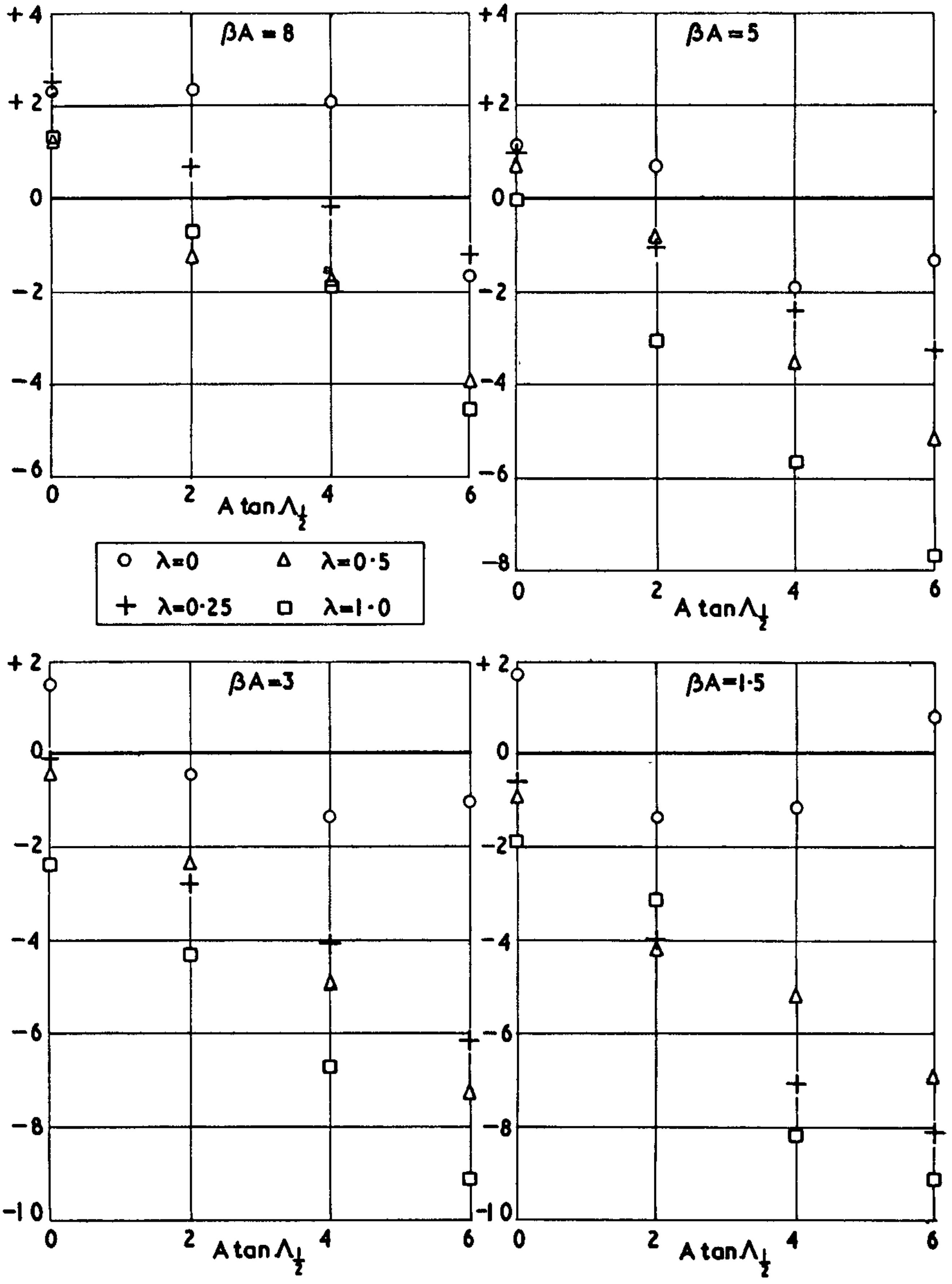

Estimated percentage errors in $\partial C_L/\partial\alpha$ from data sheet (64 wings)

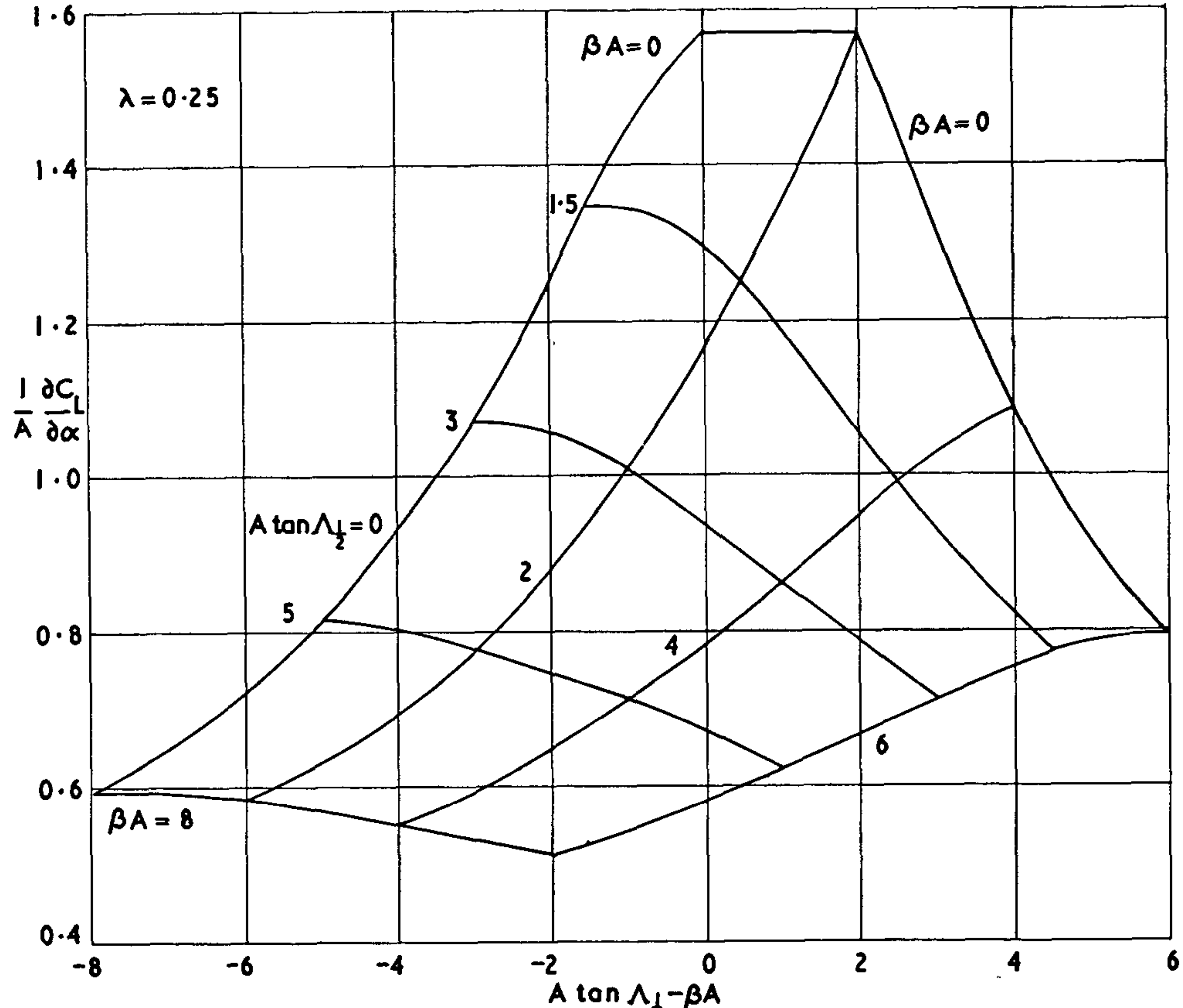

Carpet of theoretical lift slope (λ = 0·25)

FIG. 3

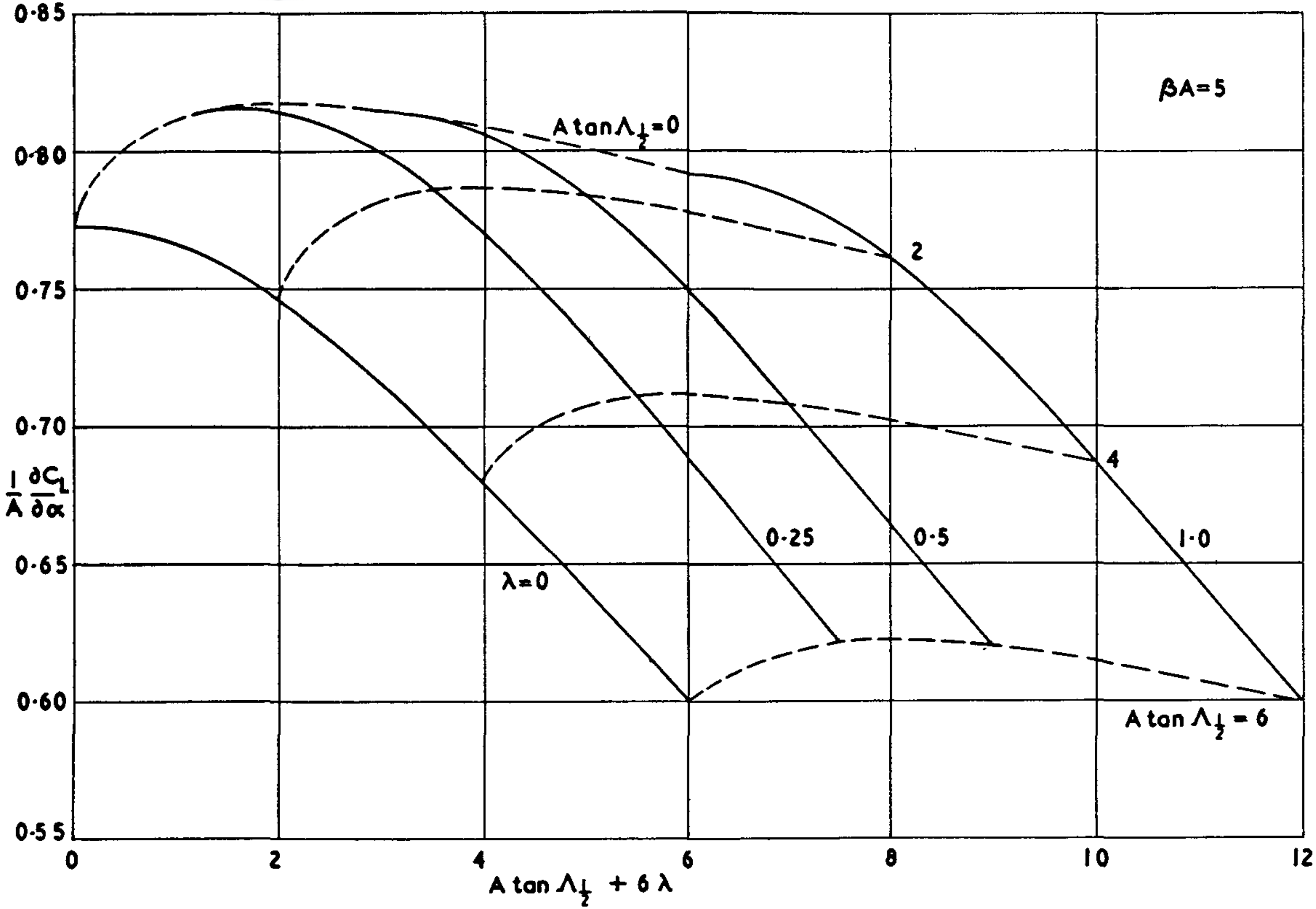

Carpet of theoretical lift slope ($\beta A=5$)

FIG. 4

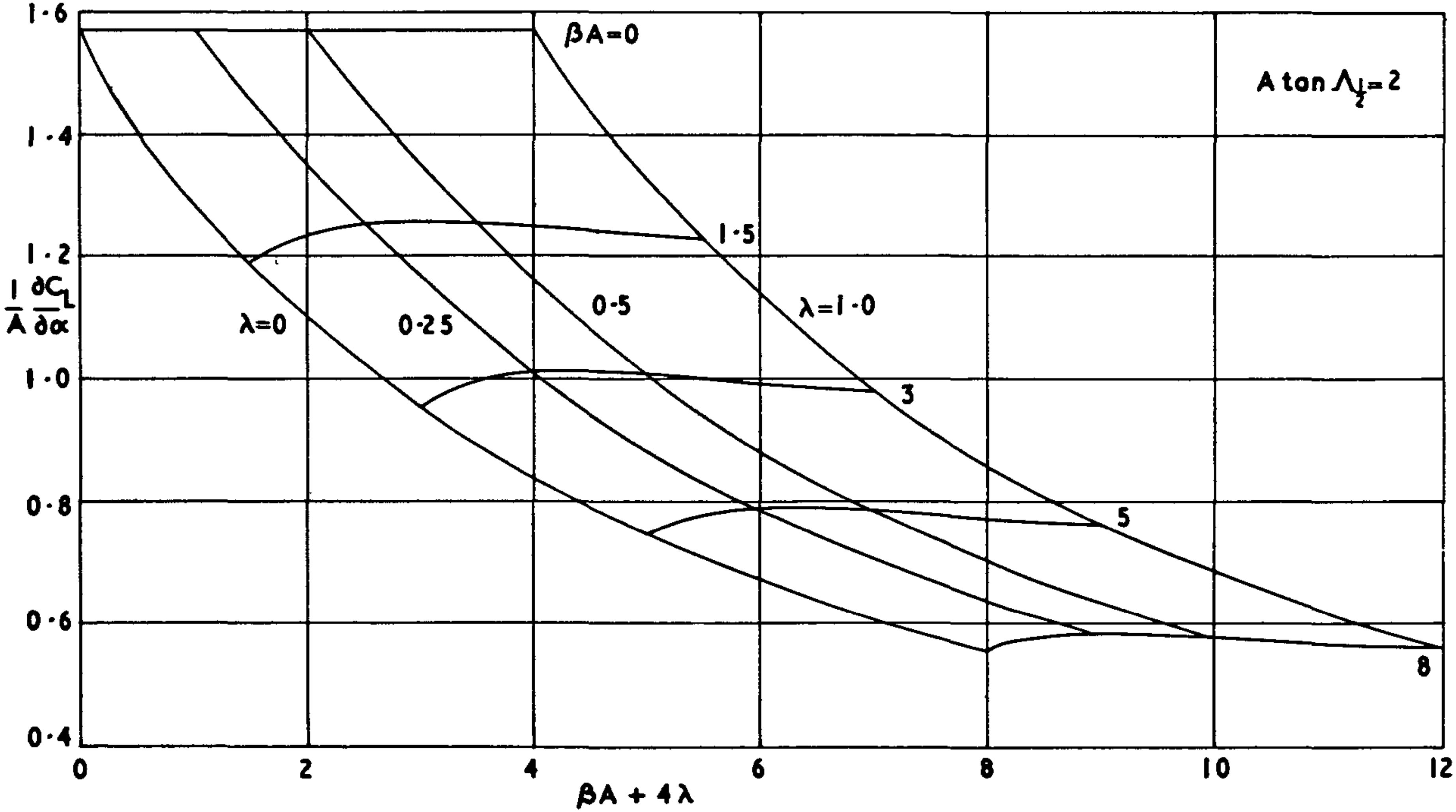

FIG. 5

Carpet of theoretical lift slope (A tan $\Lambda_{\frac{1}{2}}$ = 2)

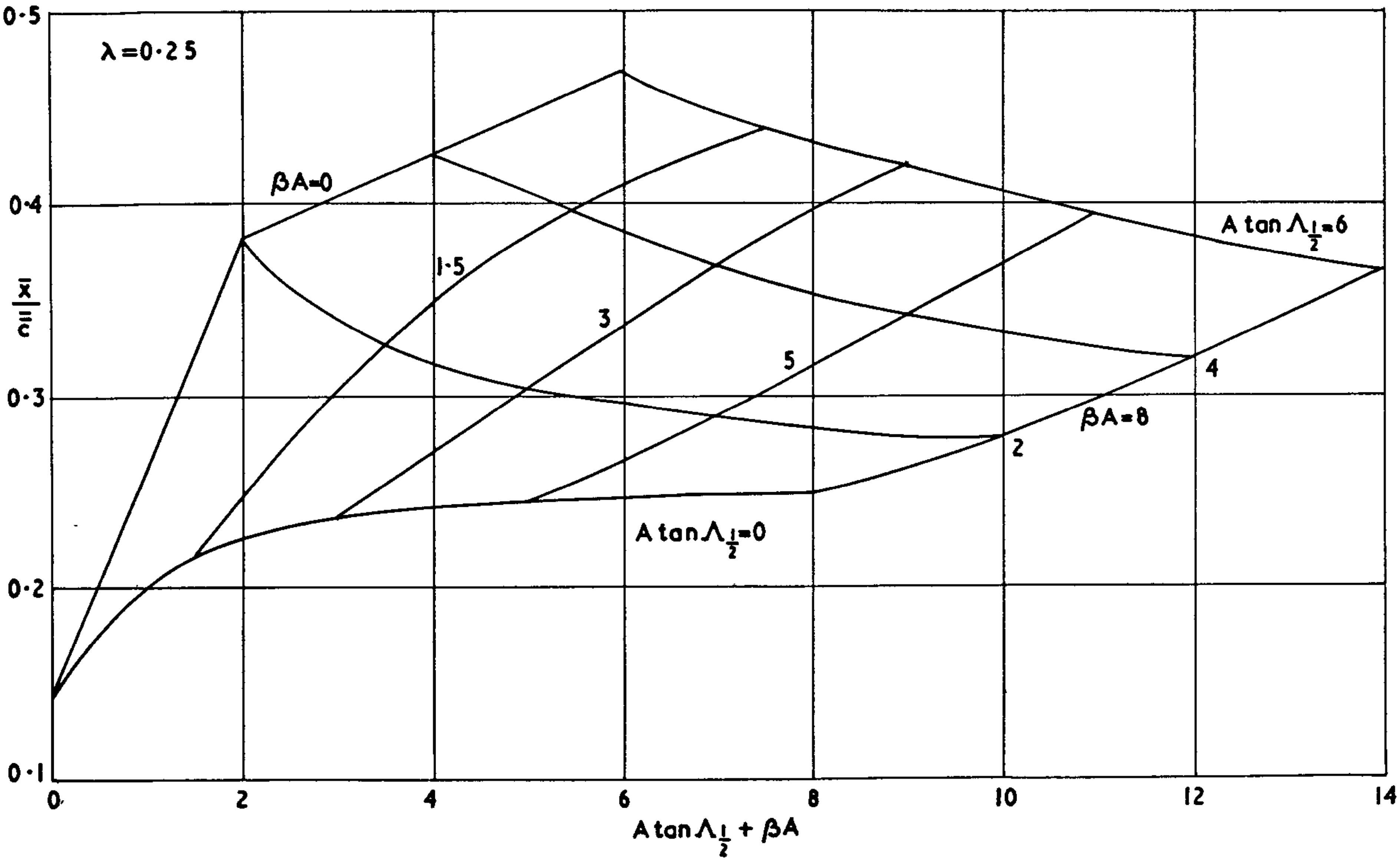

Carpet of theoretical aerodynamic centre ($\lambda = 0{\cdot}25$)

FIG. 6

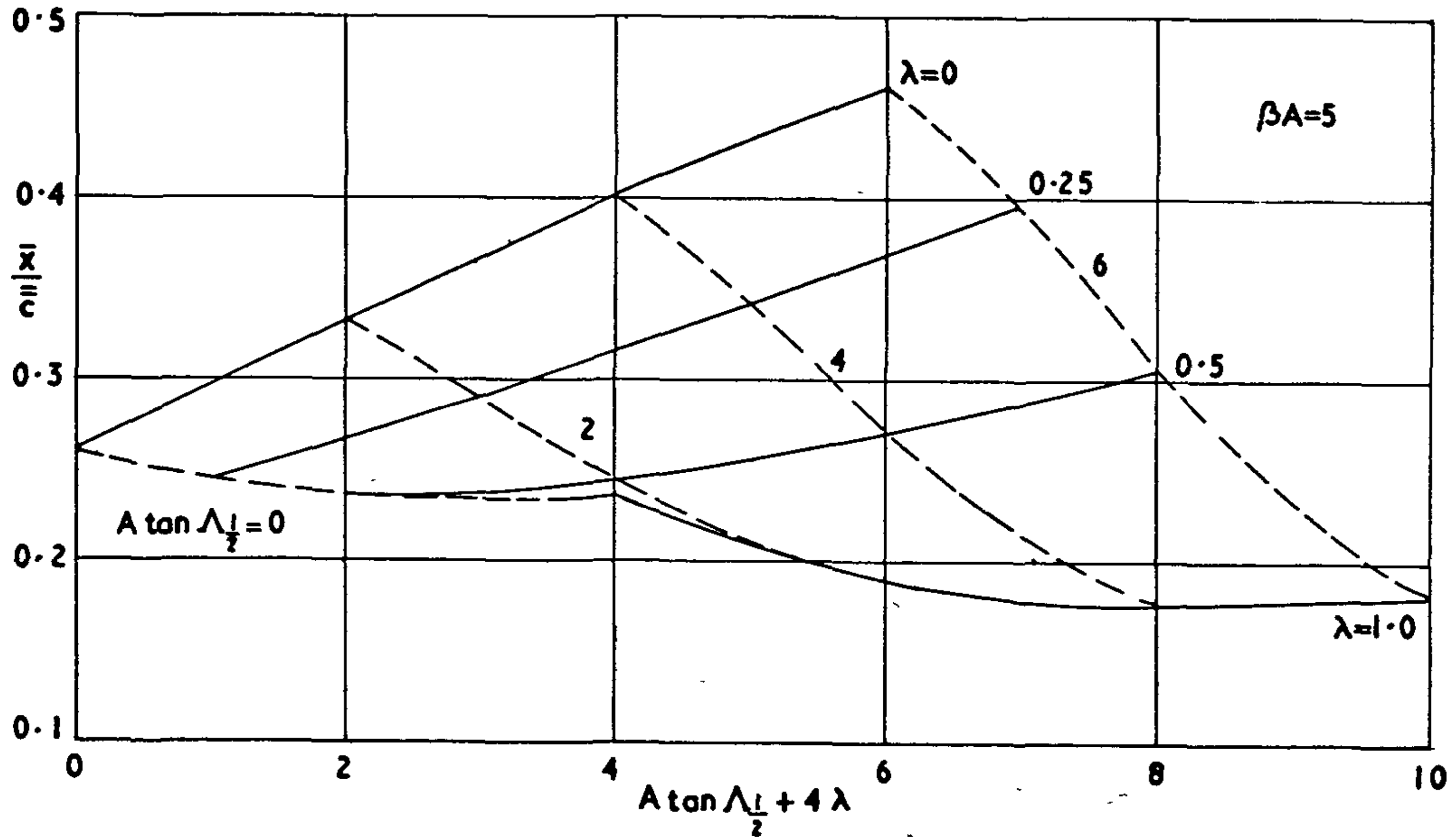

Carpet of theoretical aerodynamic centre (β A = 5)

FIG.7

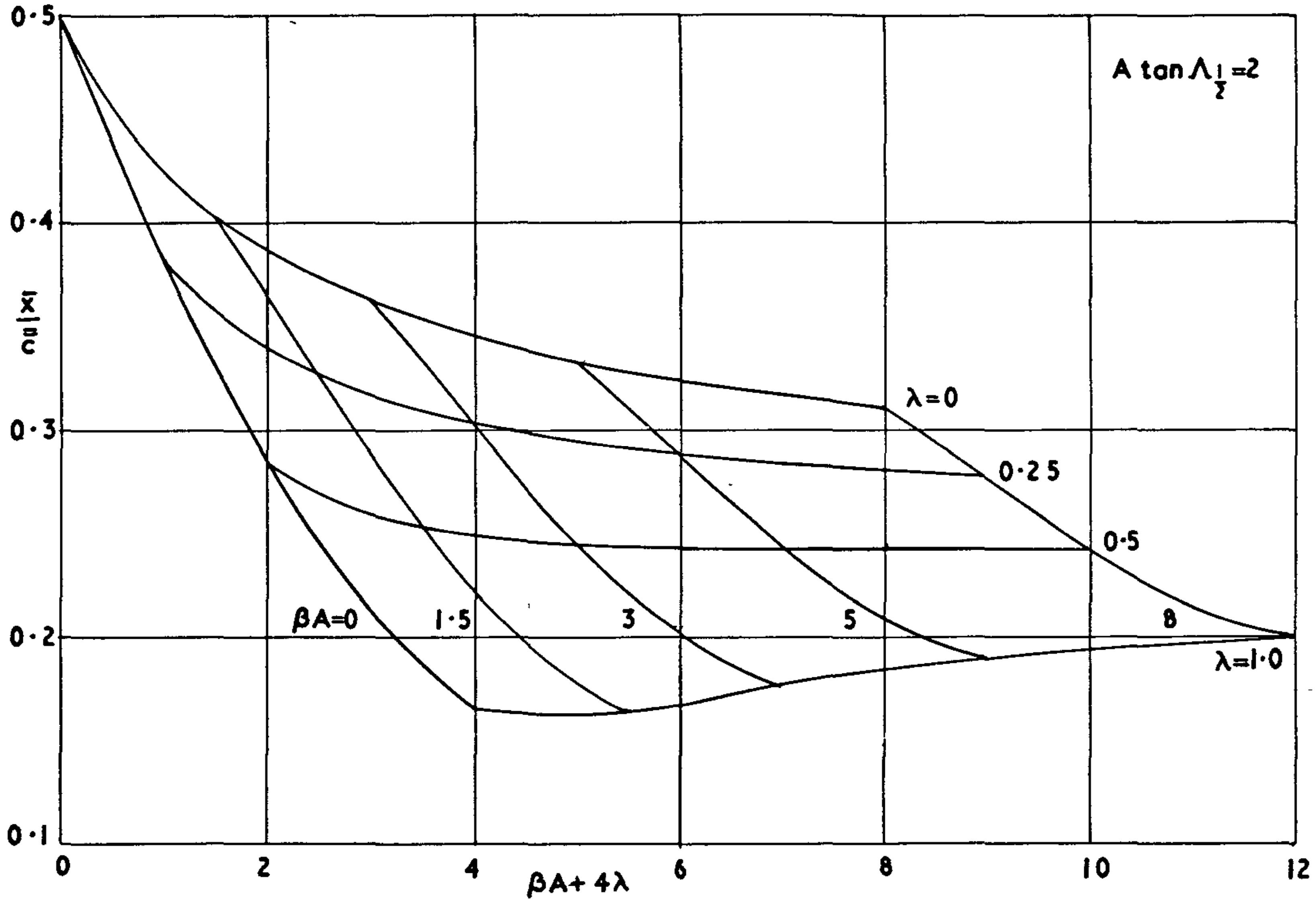

Carpet of theoretical aerodynamic centre (A tan $\Lambda_{\frac{1}{2}}$ = 2)

FIG.8

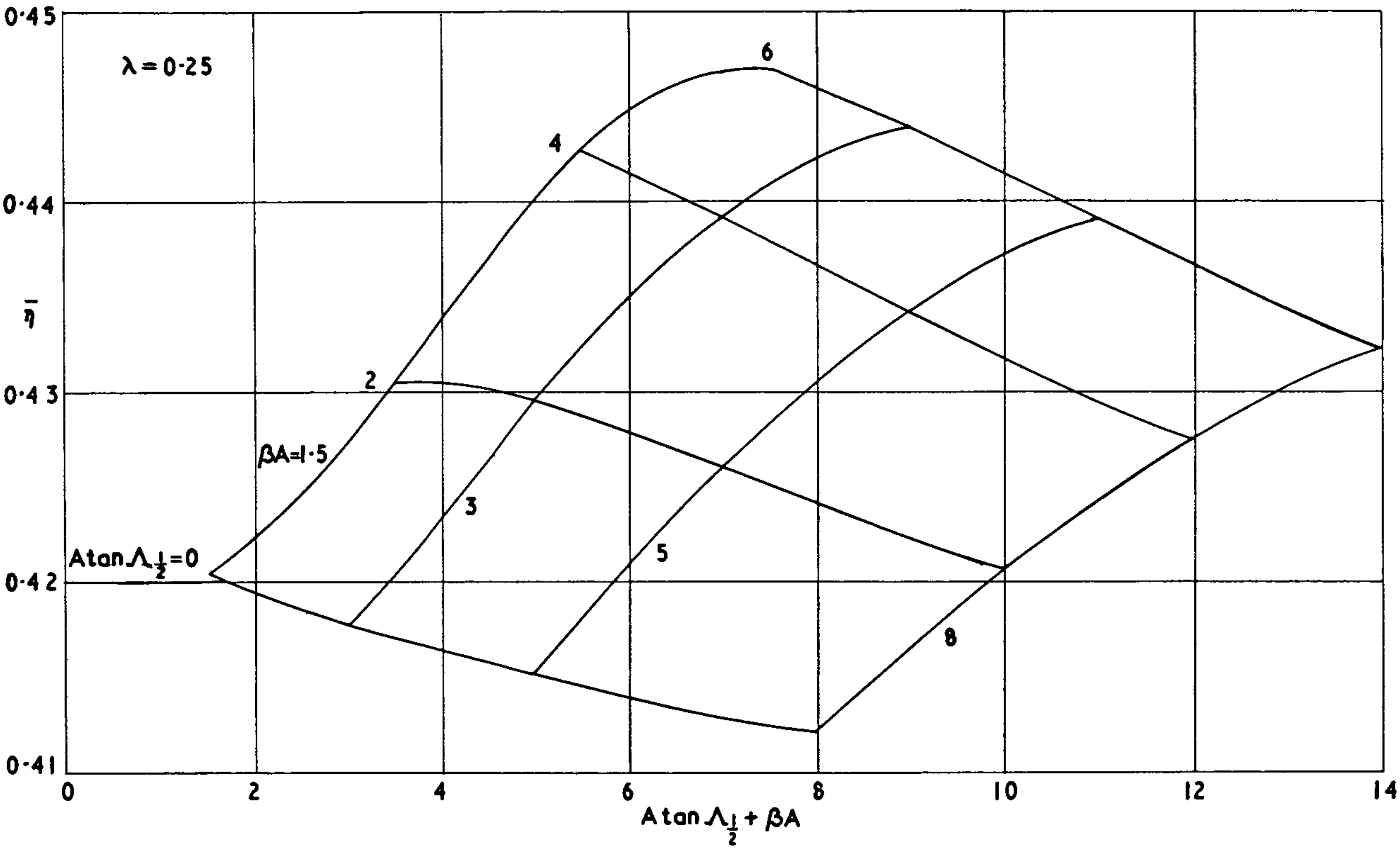

FIG. 9

Carpet of theoretical spanwise centre of pressure (λ = 0·25)

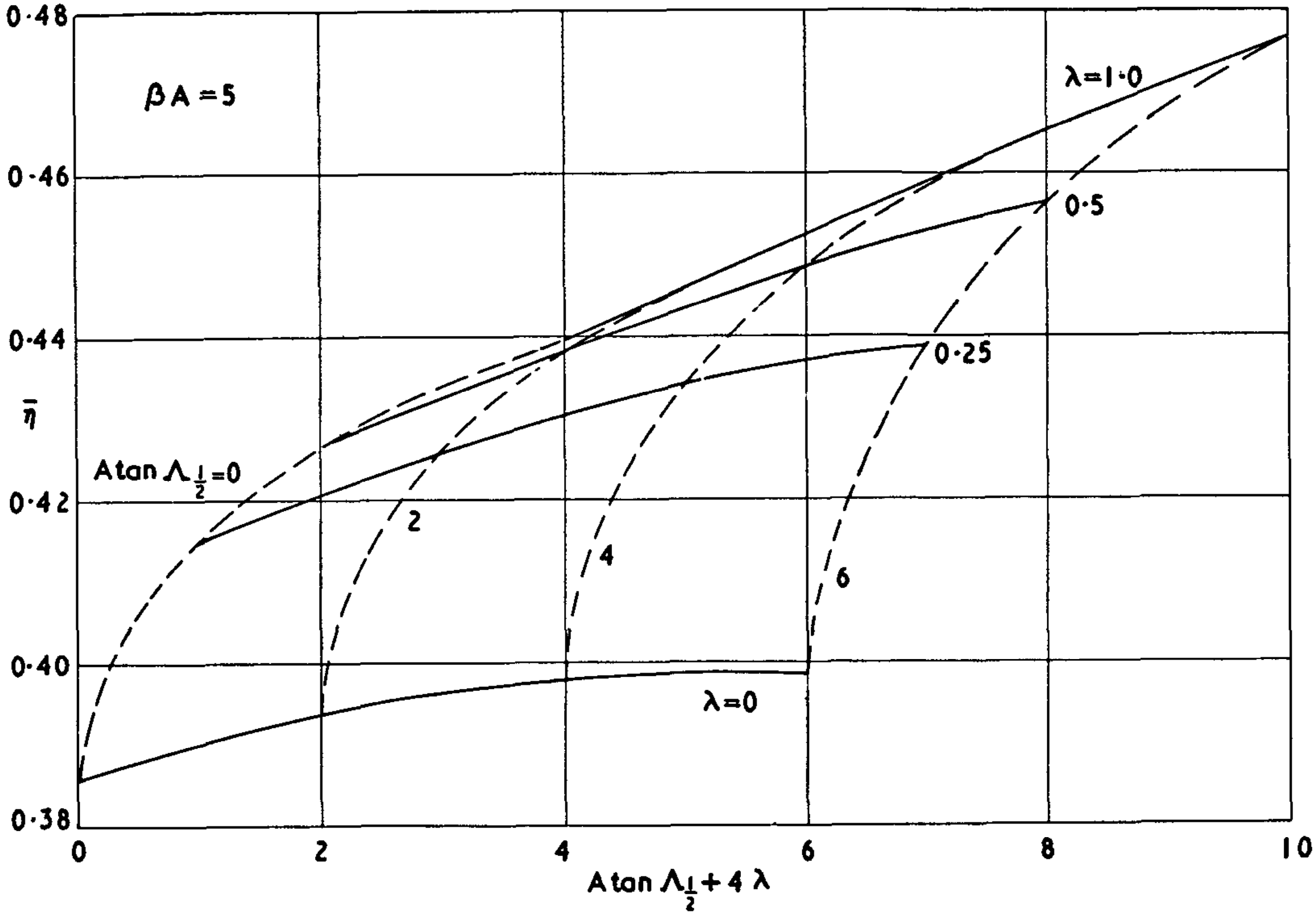

Carpet of theoretical spanwise centre of pressure ($\beta A = 5$)

FIG.10

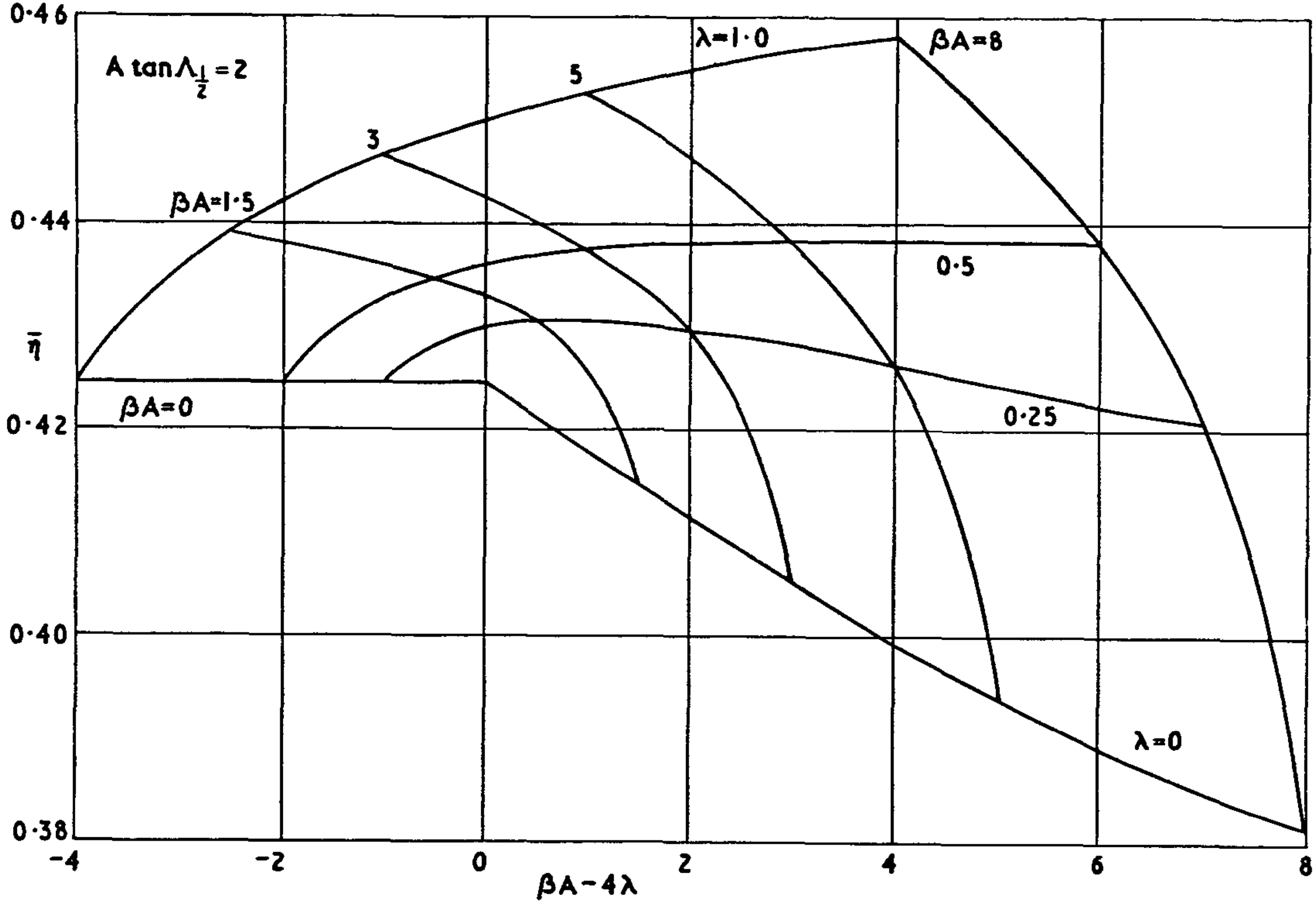

Carpet of theoretical spanwise centre of pressure ($A \tan \Lambda_{\frac{1}{2}} = 2$)

FIG. 11

FIG 12

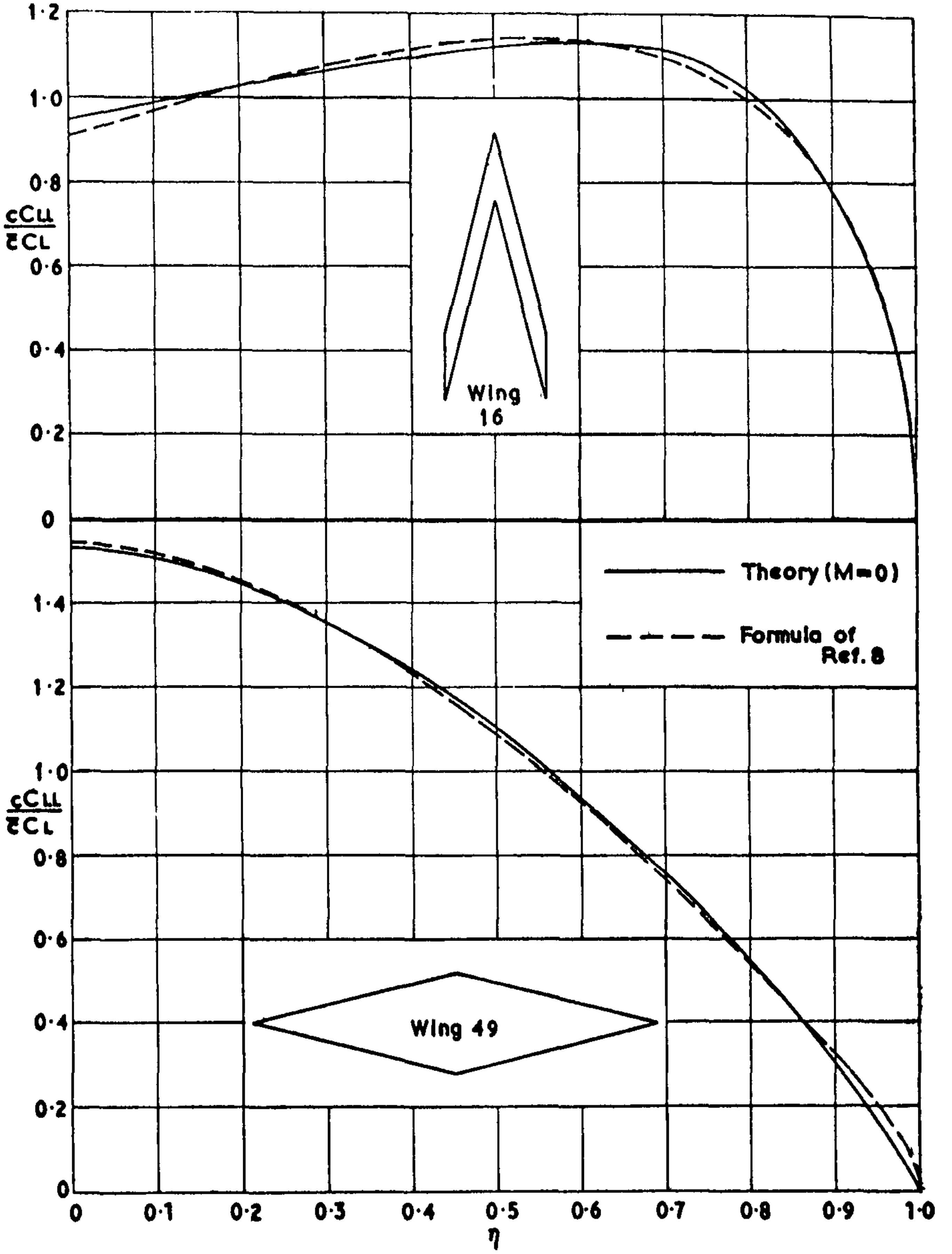

Comparisons of spanwise loading on wings of extreme planform

A.R.C. C.P. No.1137
May 1970
Garner, H. C. and Inch, Sandra M.

SUBSONIC THEORETICAL LIFT-CURVE SLOPE, AERODYNAMIC CENTRE AND SPANWISE LOADING FOR ARBITRARY ASPECT RATIO, TAPER RATIO AND SWEEPBACK

Solutions by lifting-surface theory are tabulated for 64 planforms with systematic variation in aspect ratio, taper ratio and sweepback. The accuracy of existing data sheets is examined. With the aid of sonic theory and the usual similarity rules, alternative graphical presentations of the new data are discussed. A simple relationship between trailing-vortex drag and spanwise centre of pressure is accurate to about 1%.

A.R.C. C.P. No.1137
May 1970
Garner, H. C. and Inch, Sandra M.

SUBSONIC THEORETICAL LIFT-CURVE SLOPE, AERODYNAMIC CENTRE AND SPANWISE LOADING FOR ARBITRARY ASPECT RATIO, TAPER RATIO AND SWEEPBACK

Solutions by lifting-surface theory are tabulated for 64 planforms with systematic variation in aspect ratio, taper ratio and sweepback. The accuracy of existing data sheets is examined. With the aid of sonic theory and the usual similarity rules, alternative graphical presentations of the new data are discussed. A simple relationship between trailing-vortex drag and spanwise centre of pressure is accurate to about 1%.

A.R.C. C.P. No.1137
May 1970
Garner, H. C. and Inch, Sandra M.

SUBSONIC THEORETICAL LIFT-CURVE SLOPE, AERODYNAMIC CENTRE AND SPANWISE LOADING FOR ARBITRARY ASPECT RATIO, TAPER RATIO AND SWEEPBACK

Solutions by lifting-surface theory are tabulated for 64 planforms with systematic variation in aspect ratio, taper ratio and sweepback. The accuracy of existing data sheets is examined. With the aid of sonic theory and the usual similarity rules, alternative graphical presentations of the new data are discussed. A simple relationship between trailing-vortex drag and spanwise centre of pressure is accurate to about 1%.

DETACHABLE ABSTRACT CARDS

C.P. No. 1137

Printed and published by
HER MAJESTY'S STATIONERY OFFICE

To be purchased from
49 High Holborn, London WC1V 6HB
13a Castle Street, Edinburgh EH2 3AR
109 St Mary Street, Cardiff CF1 1JW
Brazennose Street, Manchester M60 8AS
50 Fairfax Street, Bristol BS1 3DE
258 Broad Street, Birmingham B1 2HE
7 Linenhall Street, Belfast BT2 8AY
or through booksellers

Printed in England

C.P. No. 1137

SBN 11 470385 X